Y.A.S. SALEH

SIMULATION BASED INVESTIGATION OF BUILDING INTEGRATED COMBINED HELICAL AIRFOIL WITH ICEWIND BLADES OF A VERTICAL AXIS WIND TURBINE

THE GRADUATE SCHOOL OF NATURAL AND APPLIED SCIENCES
OF
ATILIM UNIVERSITY

YOUSIF ABED SALEH SALEH

A MASTER OF SCIENCE THESIS
IN
THE DEPARTMENT OF MECHANICAL ENGINEERING

JUNE 2025

ATILIM UNIVERSITY 2025

SIMULATION BASED INVESTIGATION OF BUILDING INTEGRATED COMBINED HELICAL AIRFOIL WITH ICEWIND BLADES OF A VERTICAL AXIS WIND TURBINE

A THESIS SUBMITTED TO
THE GRADUATE SCHOOL OF NATURAL AND APPLIED SCIENCES
OF
ATILIM UNIVERSITY

BY

YOUSIF ABED SALEH SALEH

IN PARTIAL FULFILLMENT OF THE REQUIREMENTS
FOR
THE DEGREE OF MASTER OF SCIENCE
IN
THE DEPARTMENT OF MECHANICAL ENGINEERING

JUNE 2025

Approval of the Graduate School of Natural and Applied Sciences, Atılım University.

Prof. Dr. Ender Keskinkılıç
Director

I certify that this thesis satisfies all the requirements as a thesis for the degree of **Master of Science in Mechanical Engineering, Atılım University**.

Prof. Dr. Sadık Engin Kılıç
Head of Department

This is to certify that we have read the thesis SIMULATION BASED INVESTIGATION OF BUILDING INTEGRATED COMBINED HELICAL AIRFOIL WITH ICEWIND BLADES OF A VERTICAL AXIS WIND TURBINE submitted by YOUSIF ABED SALEH SALEH and that in our opinion it is fully adequate, in scope and quality, as a thesis for the degree of Master of Science.

Assoc Prof. Dr. Cihan Turhan
Supervisor

Examining Committee Members:

Asst. Prof. Dr. Gizem Nur Bulanık Durmuş
Energy Systems Eng. Department, Atılım University

Assoc Prof. Dr. Cihan Turhan
Energy Systems Eng. Department, Atılım University

Asst. Prof. Dr. Bahram Lotfi
Mechanical Eng. Department, TOBB University of Economics and Technology

Date: *June 10, 2025*

I hereby declare that all information in this document has been obtained and presented in accordance with academic rules and ethical conduct. I also declare that, as required by these rules and conduct, I have fully cited and referenced all material and results that are not original to this work.

Name, Last Name: Yousif Abed Saleh, SALEH

Signature:

ABSTRACT

SIMULATION BASED INVESTIGATION OF BUILDING INTEGRATED COMBINED HELICAL AIRFOIL WITH ICEWIND BLADES OF A VERTICAL AXIS WIND TURBINE

Saleh, Yousif Abed Saleh
MSc., Department of Mechanical Engineering
Supervisor: Assoc Prof. Dr. Cihan Turhan

June 2025, 74 pages

Vertical axis wind turbine (VAWT) is one type of wind machine, which is used now a day these designs to improve the performance of the wind turbines. The main drawback when using helical airfoil blades is their low starting torque at the beginning of VAWT operation. Integrated helical airfoil with another blade shape such as (IceWind blades) helping to solve the low torque problem. In this thesis, the numerical investigation is conducted to improve the aerodynamic characteristics of the proposed design for the six-blade VAWT. Shear Stress Transport SST k-ω Turbulence Model and Finite Volume Method are used for the numerical simulation using the Ansys Fluent software. The developed model is integrated into a case building in a temperate climate zone and the energy consumption of the building is reduced by the proposed model. DesignBuilder software was used for energy consumption calculations. Among the three tested configurations, the third case showed the best performance, achieving a 30.88% reduction in energy consumption with a 10.49-year payback period.

Keywords: IceWind Turbine, Helical Wind Turbine, Vertical Axis Wind Turbine, Energy Consumption, Residential Buildings, Payback Period.

ÖZ

BİNALARA ENTEGRE EDİLMİŞ HELİKAL AEROFOİL PROFİLLİ VE ICEWİND TİPİ TÜRBİN KANATLARIYLA BİRLEŞTİRİLMİŞ DİKEY EKSENLİ RÜZGAR TÜRBİNİNİN SİMÜLASYON TABANLI ANALİZİ

Saleh, Yousif Abed Saleh
Yüksek Lisans, Makine Mühendisliği Bölümü
Tez Yöneticisi : Doç. Dr. Cihan Turhan

Haziran 2025, 74 sayfa

Dikey eksenli rüzgar türbini (VAWT), performansını artırmak amacıyla günümüzde geliştirilen ve optimize edilen bir rüzgar enerjisi sistemidir. Bu sistemlerde helikal aerofoil profilli kullanılmasının başlıca dezavantajlarından biri, türbinin ilk çalışma aşamasında düşük kalkış torku üretmesidir. Helikal aerofoil profilinin IceWind tipi türbin kanatları gibi başka bir kanat geometrisiyle entegre edilmesi, düşük tork sorununu çözmeye yardımcı olmaktadır. Bu tez kapsamında altı türbin kanadına dikey sahip eksenli rüzgar türbini VAWT tasarımı için aerodinamik özellikleri iyileştirmeye yönelik nümerik bir analiz gerçekleştirilmiştir. Nümerik simülasyonlar, Ansys Fluent yazılımı kullanılarak Kayma Gerilmeli Taşınım türbülans (Shear Stress Transport – SST) k-ω modeli ve Sonlu Hacim Yöntemi ile gerçekleştirilmiştir. Geliştirilen model, ılıman iklim kuşağında yer olan örnek bir binaya entegre edilmiştir ve bu yenilikçi model sayesinde binanın enerji tüketimi azaltılmıştır. Enerji tüketimi hesaplamalarında DesignBuilder yazılımı kullanılmıştır. Test edilen üç yapılandırma arasında, üçüncü senaryo en iyi performansı göstermiş ve enerji tüketiminde %30,88 oranında azalma sağlanmış ve geri ödeme süresi 10,49 yıl olarak hesaplanmıştır.

Anahtar Kelimeler: IceWind Türbini, Helikal Rüzgar Türbini, Dikey Eksenli Rüzgar Türbini, Enerji Tüketimi, Konut Binaları, Geri Ödeme Süresi.

To my family and my advisor

ACKNOWLEDGMENTS

I am sincerely thankful to my advisor, Assoc. Prof. Dr. Cihan Turhan, for his continuous support throughout my MSc. Journey. His patience, encouragement, and profound knowledge have been a great source of guidance. His valuable assistance was crucial during every stage of this research and the writing of this thesis. This work could not have been completed without his supervision and support. I also extend my appreciation to my thesis committee members, Asst. Prof. Dr. Bahram Lotfi and Asst. Prof. Dr. Gizem Nur Bulanık Durmuş, for their helpful feedback and constructive feedback.

Finally, I would like to express my gratitude to my father, mother, and brother of their constant support and love, which gave me the strength to overcome every challenge throughout this journey.

TABLE OF CONTENTS

LIST OF TABLES

LIST OF FIGURES

FIGURES

LIST OF SYMBOLS AND ABBREVIATIONS

Symbols	**Description**
N	Number of Blades
c	Chord Length
D	Rotor Diameter
H	Rotor Height
V	Wind Velocity
ω	Angular Velocity
ρ	Air Density
P	Pressure
$P_{Turbine}$	Power Output
A_S	Swept Area
R	Radius of The Rotor

Abbreviations	**Description**
VAWT	Vertical Axis Wind Turbine
HAWT	Horizontal Axis Wind Turbine
CFD	Computational Fluid Dynamics
3D	Three Dimensions
2D	Two Dimensions
RANS	Reynolds-Averaged Navier Stokes
SST	Shear Stress Transport
BAWT	Building Augmented Wind Turbines
SWT	Small Wind Turbines
HCAWT	Helical Cross Axis Wind Turbine
TS	Turkish Standard
EPS	Expanded Polystyrene
NACA	The National Advisory for Aeronautics
TSR	Tip Speed Ratio

CHAPTER 1

INTRODUCTION

In this section, the importance of building in terms of energy consumption and the need of renewable energy, the wind turbine portion as a renewable energy source will be given.

1.1 Energy Consumption in Buildings

Energy consumption is considered one of the most important problems that the world suffers at these days, and most countries use sort of integrated methods to increase energy efficiency, especially with regard to energy consumption in buildings, as buildings constitutes 40% of the total energy consumption, and this ratio is considered a high percentage compared to other fields such as transportation, industrial and agricultural energy consumption etc. [1].

If one can see the latest breakdown of buildings energy use statistics for Türkiye, as shown in (Figure 1.1), the percentages of non-renewable energy and renewable energy consumption in residential buildings for natural gas and electricity is 49% and 22%, respectively. Even the researchers notice a reduction in the use of coal, the percentage of renewable energy consumption is still 14% in Türkiye [2].

As a result of the rapid growth of the population and the increase in demand for the construction of residential buildings, as previous studies showed that between the years 2000 and 2017, the demand for energy in buildings increased by 20%. This ratio indicates an increase in energy consumption in the coming years, which made countries take paths and plans to construct buildings equipped with renewable energy technologies. Therefore, renewable energy technologies support increasing the use of clean electrical energy and improving the energy efficiency of the buildings [3].

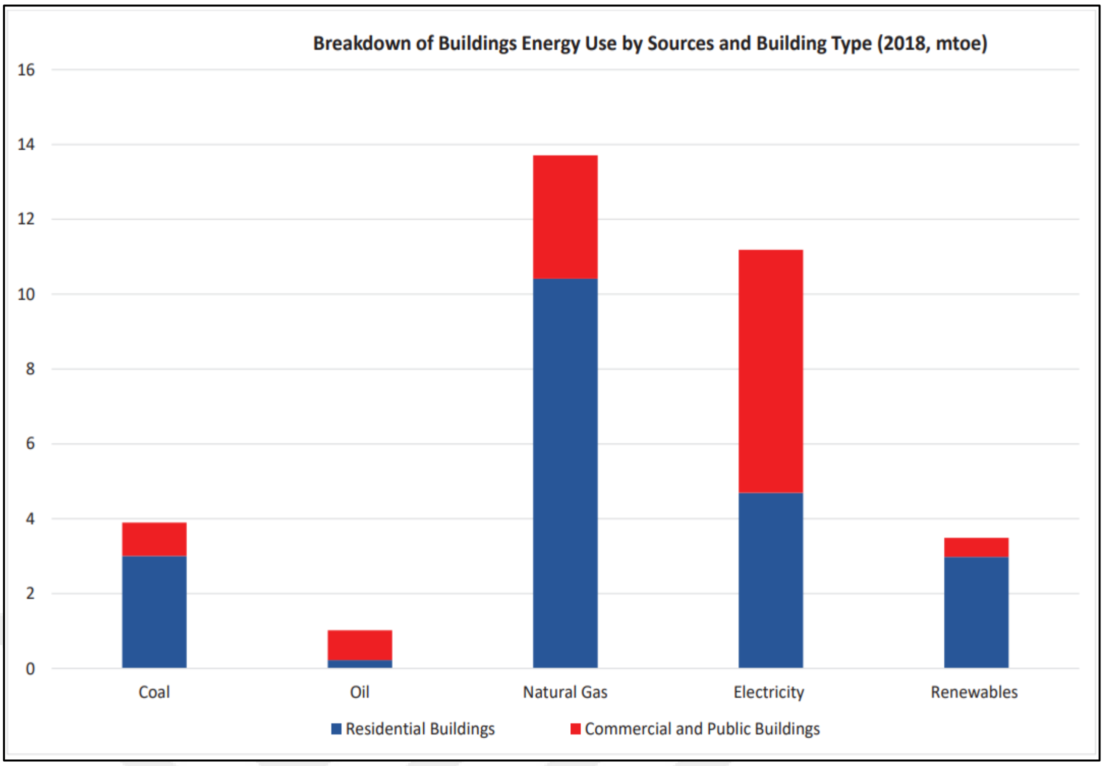

Figure 1.1 Breakdown of Buildings Energy Use by Sources and Building Type (2018, mote) [2]

Natural energy resources are among the most important sources that countries depend on in their sustainable development. Today, developed countries have invested their natural resources, however these countries have integrated renewable and non-renewable energy efficiently. Due to the continuous decline in non-renewable energy sources, meeting energy needs become difficult day by day, so studies are now being constantly conducted in order to find the most efficient renewable energy technologies, including wind energy, solar energy, hydroelectric energy, geothermal energy and bioenergy [4].

One of the methods adopted to reduce energy consumption of building is wind energy, where small-scale wind turbines are installed, either horizontally or vertically, on the roofs of the building. These turbines are called Building Augmented Wind Turbines (BAWT) as shown in (Figure 1.2) [5].

Contributing to improving energy efficiency in residential buildings has a great benefit in reducing harmful non-climate impacts and conducive to reduce energy costs.

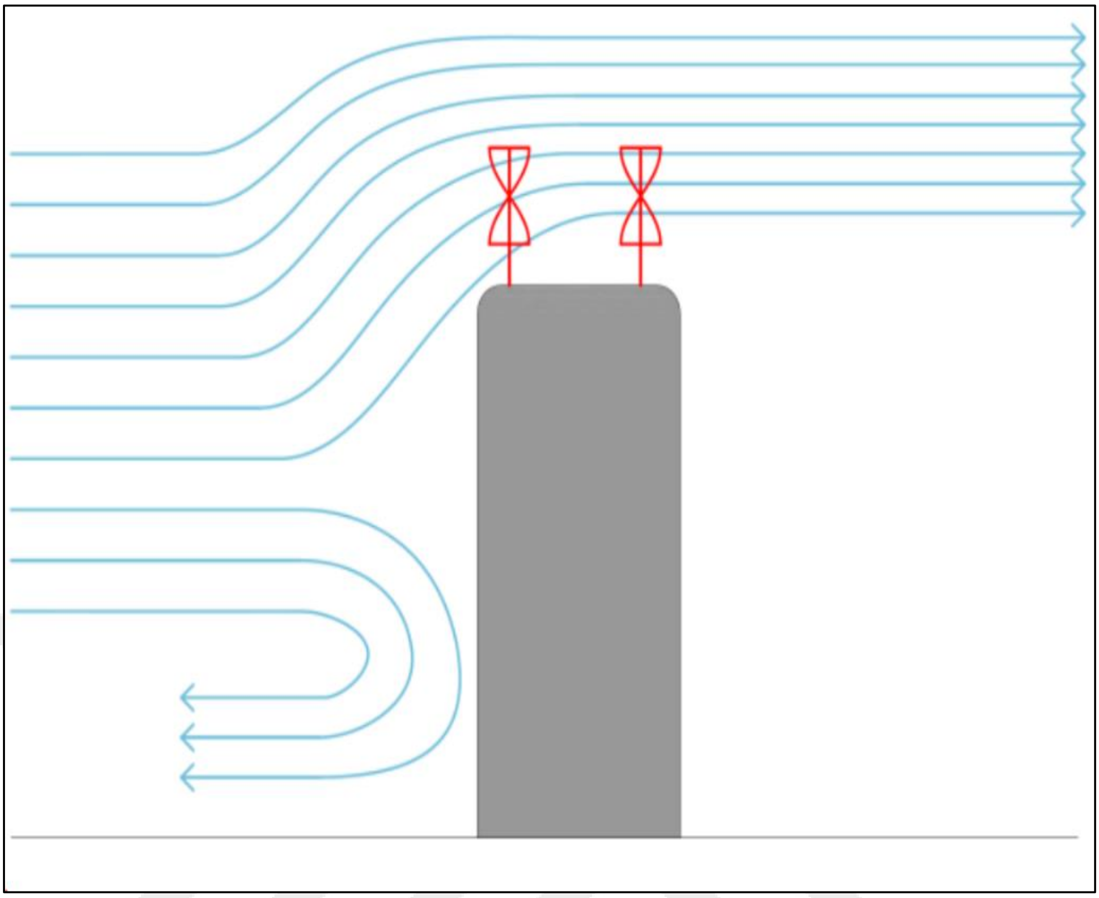

Figure 1.2 BAWT in The Rooftop Mounted [5]

1.2 Renewable Energy as a Wind Power

Wind energy is one of the types of renewable energy sources that can be used via wind turbines. Wind speed plays an essential role in choosing the appropriate area for using wind turbines [4].

According to geographical maps, there are very limited areas which are suitable for designing and constructing wind turbines, for example, when we see the geographical map for the distribution of wind energy in Türkiye (Figure 1.3), the yearly wind speed range is from a low 2.1 m/s in the East Anatolia district to a high of 3.3 m/s in the Marmara district because in large portion of these areas wind speed exceeds 3 m/s, these two areas are considered among the best suitable regions in Türkiye in the field of wind energy generation [6].

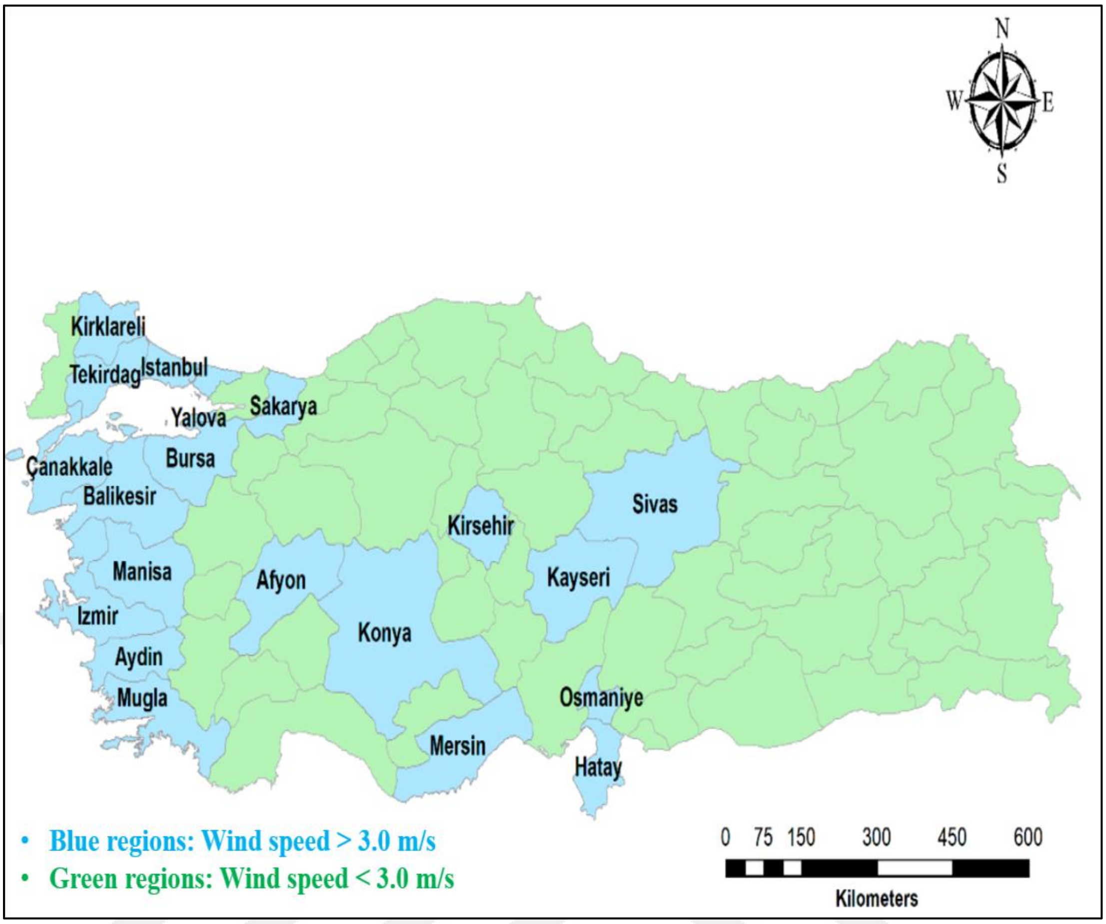

Figure 1.3 Geographical Distribution of the Provinces within the Top Twenty in Terms of Installed Wind Power Capacity in Türkiye [4]

Low costs and non-carbon emissions are among the most important features of this type of energy, which makes it friendly to the climate and the environment. Therefore, wind turbines can be used as a source of generating electrical energy. Nowadays, the global focus is on converting wind energy using different types of horizontal and vertical axis wind turbines [7].

1.3 Wind Turbines

Over the past periods, wind energy has been adopted as a primary and rapid source for developing renewable energy. At first, wind energy systems were used by farmers and institution in the form of Small Wind Turbines (SWT), over time wind turbines became used on the roofs of residential buildings which was developed by engineers specialized in energy and architectural design, taking into account the shape of the roof and the height of the building because they are among the factors affecting this type of turbine [8].

Many types of small-sized turbines are used on the top of buildings, including the Savonius type due to its simple design, and the Darrieus type is considered one of the desirable options for installing it on the roofs of buildings because of low-level acoustic emission. VAWTs are used on the roofs of buildings due to their multidirectional capacity in turbulent flow [9].

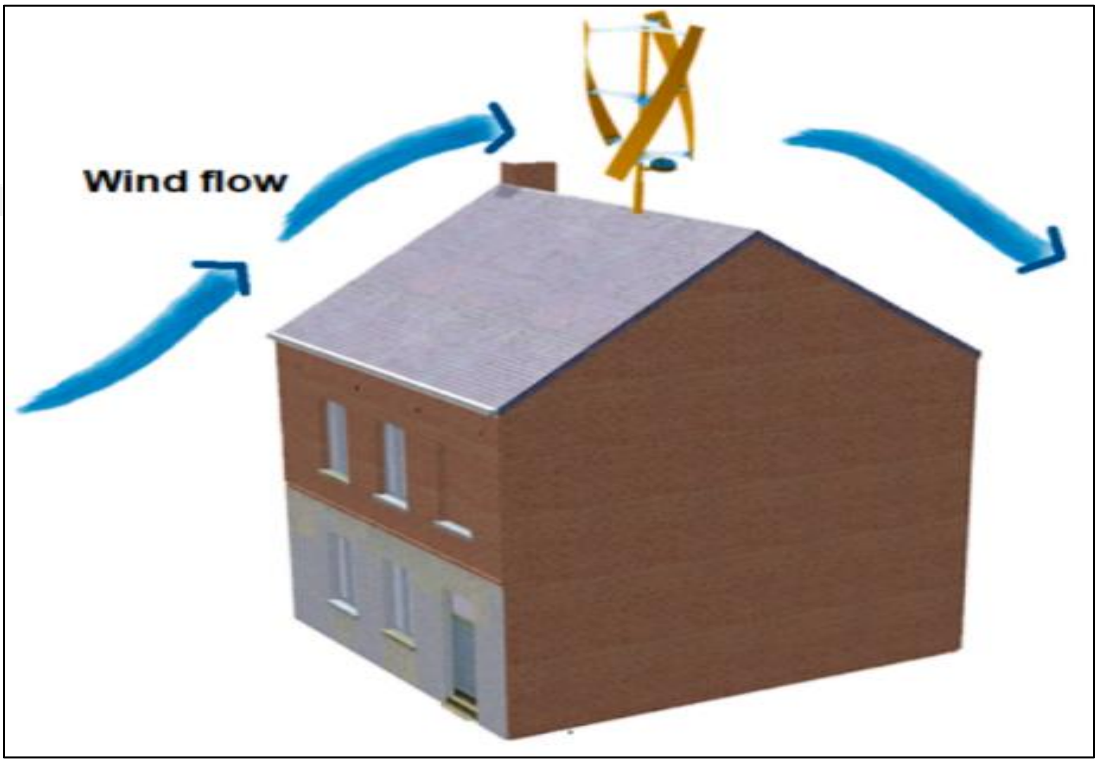

Figure 1.4 Schematic Diagrams of Conventional Small-Scale VAWT Installed on the Roof of a Building [9]

1.3.1 Types of Building-Integrated Wind Turbines

A building-integrated wind turbine can be divided into two main parts: power capacity and axis of rotation or can classified as rotor diameter (m) and power rating (kW) [10]. The rotation axis can be divided into two parts: Vertical Axis Wind Turbine VAWT and Horizontal Axis Wind Turbine shown in (Figure 1.5). The HAWT is a turbine whose axis of rotation is horizontal and perpendicular to the direction of the wind [11], when in the VAWT, the basic components are at the base of the turbine, while the vertical axis will be adjusted so that it is tangential to the wind. In this type of wind turbine, there is no need for wind sensing because the wind turbines can capture the wind from all directions. The blade is one of the essential parts of a wind turbine and must be carefully designed in order to achieve higher energy efficiency. The Darrieus type considered lift-based, its generated by airfoil's shape to create a pressure between upper and lower surfaces, bringing about perpendicular upward force to the direction of the wind, the Darrieus is considered one of the best types of vertical turbines because it has a simple operating principle and high efficiency, but this type requires an external energy source to start rotation due to the low torque. As for the Savonius type, it is considered drag-based, its mean parallel force to flow direction, also produced by the blades when they move through the air. We also have H-rotor turbine which has multiple designs: Tilted, Helical H-rotor and Articulating [10].

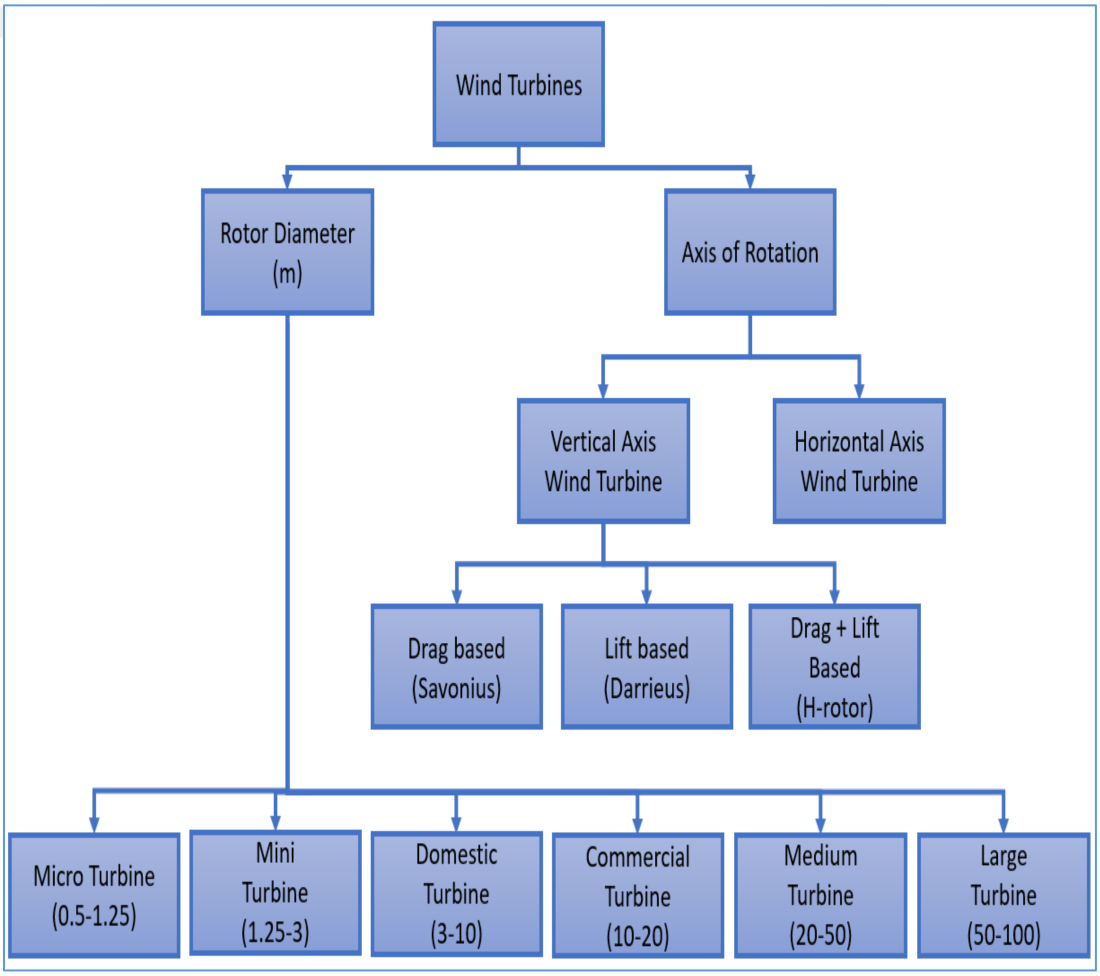

Figure 1.5 Types of Wind Turbines (adapted from [10])

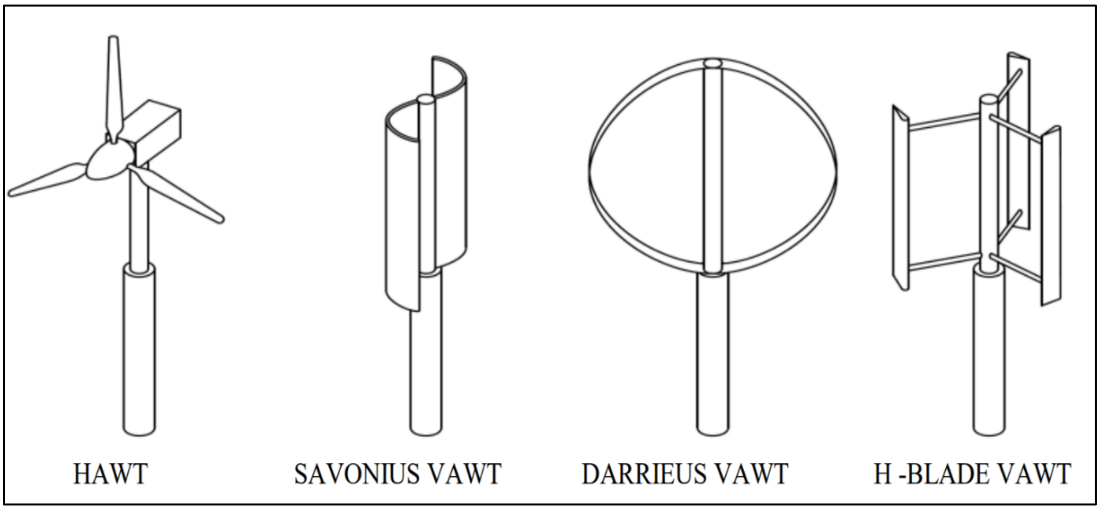

Figure 1.6 Different Types of Wind Turbine [10]

1.3.2 Advantages and Disadvantages of the VAWTs Compared to HAWTs

The VAWTs are more likely to be used over HAWTs for several main reasons shown in table 1.1.

Table 1.1 Summary of Benefits and Limitation of VAWTs

VAWTs Advantages	VAWTs Disadvantages
• There is no need to yaw mechanism (permits the turbine to turn or “yaw” to look into the oncoming wind). Additionally, VAWTs can take advantages from districts where roofs passes channel the wind and raise wind speed.	• VAWTs generally exhibit lower efficiency in contrast with typical HAWTs. This attributed to drag increasing by VAWTs as their blades rotate into the wind.
• Can be located closer the ground, making it more take part to keep up with the moving parts.	• It cannot make use of higher wind speeds above because the rotors located nearer the ground and the wind speeds are being brought down.
• VAWTs have lower startup speed than normal HAWTs.	• HAWTs are most economical compared to VAWTs because of high production cost in VAWTs, also maintenance costs.

CHAPTER 2

LITERATURE REVIEW

In this section, many approaches of passive and active solutions design strategies to reduce energy consumption in the building sector will be given in detail. Passive and active solutions will be given in the first stages. However, the main focus will be on the usage of small-scale wind turbines, which are integrated into the buildings.

Passive strategies become important methods to decrease the need for heating and cooling and lighting systems in residential buildings. Many studies have focused on building site orientation because of its role in optimizing solar exposure and enhancing natural ventilation. Residential construction materials such as brick and concrete help maintain thermal equilibrium due to the possession of high capacities to absorb and store heat energy [12]. Previously suggested solutions provided lower energy savings compared to the active solutions currently utilized. Wind turbines and PV solar panels serve as active systems that generate renewable energy. The main purpose of these strategies is to lower dependence on traditional power sources and support the development of a sustainable environment [13].

2.1 Passive Solutions

Hendinata, L. (2023) [14] investigated and simulated a high-rise apartment building in various cities in Indonesia with three window models (Single pane, double-glazed and thermochromic glass windows) by using the EnergyPlus Software. Based on this study, the authors found that replacing the single-pane and double-glazing windows could reduce total energy consumption by 10.96%. Furthermore, employing thermochromic windows instead of the clear and conventional glazed windows is more effective in reducing energy demand up to 24.19%.

Monis, M., and Rastogi, A. (2022) [15] discussed several influencing factors of passive design solutions such as thermal mass, thermal insulation, building orientation, external shading devices and window size, shape and design. High thermal mass used less energy in cold or hot climate zones compared to low-mass buildings, indicating that the building mass affects energy efficiency. Effective insulation, including material such as expanded polystyrene (EPS) and Rockwall remarkably reduces the environmental impact of energy use. Orientation plays a crucial role in decreasing energy consumption in buildings by focusing on reducing solar heat absorption in hot locations and maximizing solar gain in cold regions. Three types of shading systems were conducted: moveable shading, fixed shading, and other shading systems. The relevance of window size, position and shape for building energy efficiency, the studied suggested using an Energy Conservation Building Code (ECBC) window which decreased energy use compared to conventional window (Base Case) as shown in (Figure 2.1). Hence, ECBC defines standard for window-to-wall ratio (WWR) and Solar Heat Gain Coefficient (SHGC).

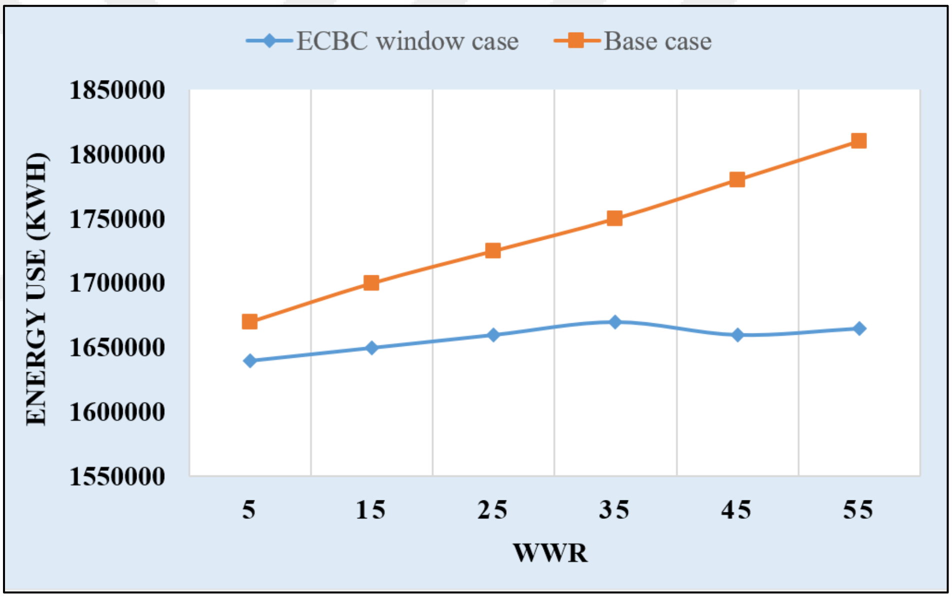

Figure 2.1 Energy Consumption for Base Case and ECBC Window Case (WWR) (reproduced from [15])

Al-Tamimi, N. (2022) [16] discussed four strategies on passive solution designs for residential buildings in hot climate zone (Saudi Arabia, Sharurah). The four aspects are: Glazing type, thermal insulation, green roof, and external shading. The study used base case (BC) of residential building then simulated these strategies separately using the DesignBuilder Software and found the use of triple low-e film glass, which can reduce energy consumption in residential buildings by 5.15% because this glazed window has a low U-value with good light transmission as shown in (Figure 2.2 a).

This study recommended the significant role of thermal insulation by using a 25mm thick thermal insulation layer which reduces energy consumption by 14.7% shown in (Figure 2.2 b). Aluminium fins, placed vertically and overhanging horizontally at 60 cm depth, could reduce energy consumption by 6.6%, as they help block solar radiation from varying sun angles. Additionally, the study showed that the green roof contributed to a 7.9% reduction in energy consumption. If applied together, these strategies can significantly decrease annual energy consumption by 35.4%.

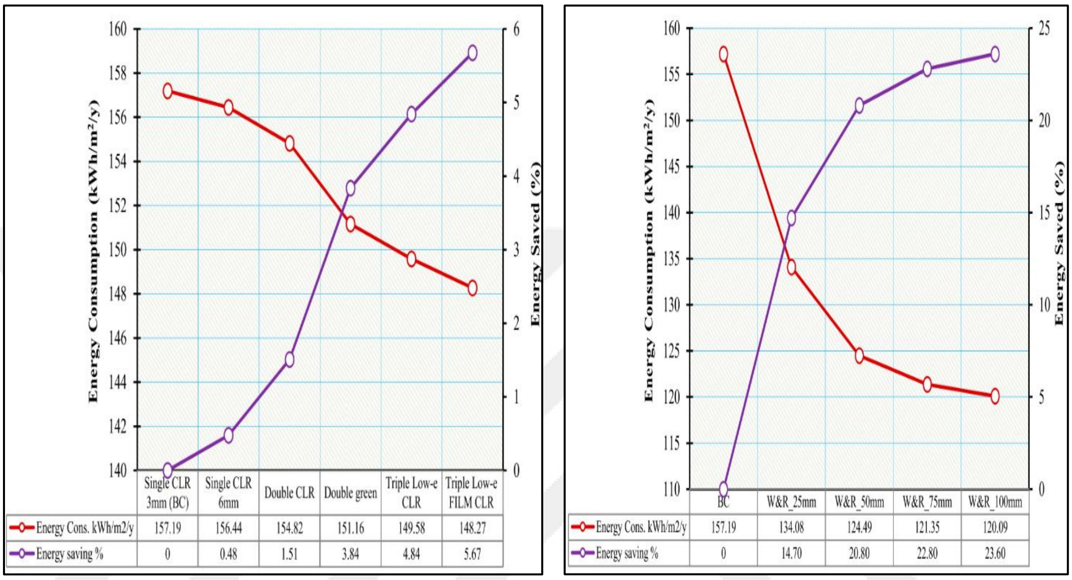

Figure 2.2 (a) Influence of Glazing Types on Energy Consumption, (b) Influence of Insulation Thickness on Energy Consumption [16]

Arsentev, A., and Rymarov, A. (2023) [17] utilized the use of phase change materials (PCM) in a one-storey dwelling located in Moscow, Russia with specific dimensions (19.9 m x 12.75 m) to reduce energy consumption for space heating and cooling by using various BioPCM materials with specific thicknesses and melting points. The simulations conducted using DesignBuilder software revealed that BioPCM M91/Q23 resulted in the lowest energy consumption with 6.3 kW for cooling and 56.14 kW for heating. Additionally, this configuration can substantially decrease heating and cooling costs.

Jaradat, M. et al. (2023) [18] investigated another case building located in Oradea, Romania, and the cities of Amman, Irbid, and Aqaba in Jordan with a two-storey residential building with a net conditioned area of 184.96 m^2. The DesignBuilder simulation tool was used to find the effect of bio-based phase change materials

(BioPCMs). At a melting point of 23°C, BioPCM M91/Q23 decreased energy consumption by 34.38% for heating and 23.33% for cooling. The overall energy saving achieved by incorporating PCM was 18.23%.

Bekele, M., Atakara, C. (2023) [19] applied passive solar and energy efficiency design strategies (PSEEDS) in two disparate residential buildings, traditional Mediterranean and contemporary houses situated in North Cyprus. Two-storey, each having an actual area of 400.98 m^2 with different construction materials and dimensions. By comparing the results between these scenarios, the authors found that the energy demand in the traditional Mediterranean house reduced by 34.71% after adopting PSEEDS, which included a glass façade, proper orientation, and the use of high thermal mass materials. On the other hand, the energy consumption in the contemporary house was reduced by about 31.38%. The research demonstrated that (PSEEDS) significantly reduces electricity consumption in both types of buildings. Despite this, the higher thermal mass of traditional Mediterranean houses contributes to their increased efficiency.

Huang, H. et al. (2020) [20] investigated a 20-storey high-rise residential building located in Jining city, Shandong province, China, through building energy simulation using the DesignBuilder software. The study aimed to apply passive strategies by adding insulation to the ground floor, roof, and windows. Moreover, vacuum insulation panels (VIP) were used. An advanced air conditioning system with a coefficient of performance (COP) replaced the coal-fired heating plant. To control solar gain, side-fins, louvres, and overhangs were implemented. The research revealed that after employing these solutions such as shading systems, HVAC upgrades and fabric retrofitting. The overall energy consumption decreased by 78.9%.

2.2 Active Solutions

Terashima, K. et al. (2023) [21] presented an environmentally friendly photovoltaic/thermal (PV/T) panel strategy for Building-Integrated Photovoltaic/Thermal (BIPVT) systems. The study used Copper-Indium-Selenium (CIS) PV module and integrated a heat exchanger coupled with flat aluminium tubes. This system converts 73.5% of solar energy into hot water at approximately 40°C with 13% power generation productivity and about 60.5% heat collection efficiency. In comparison, previous results using m-Si PV/T panels showed 45.9% solar energy conversion into hot water at around 60°C with 12% power generation performance and about 33.9% heat collection efficiency. The suggested PV/T panel shows higher efficiency and the capability of providing residential heat demands compared to traditional m-Si and CIS PV modules, while minimizing the environmental thermal load.

García-Gáfaro, C. et al. (2022) [22] investigated an active photovoltaic forced ventilated façade (PV-FVF) with adaptive indoor temperature setpoint strategy $T_{adaptive}$ to enhance energy consumption in a residential building located in Madrid, Spain. found that the $T_{adaptive}$ strategy caused a reduction of at least 19.9% in air-source heat pump (ASHP) energy consumption. In addition, when using this strategy, the coefficient of performance (COP) of the pump increased by 17.4%. The results of this study showed that heating energy consumption decreased by at least 19.9% when using the heat pump and (PV-FVF) system, coupled with an under-floor heating system led to a 20.7% reduction in annual total energy demand, encompassing Domestic Hot Water (DHW).

Aneli, S. et al. (2023) [23] performed a case study of two-storey single- family building with 70 m^2 of net area per floor, located in South Italy, examined a solar-assisted heat pump (SAHP) system strategy which included implementation of both electric (EES) and thermal (TES) energy source systems. The TRNSYS software was used as a simulation tool for analyzing the energy system. The analysis showed that having a thermal storage of about 1000 L and electrical storage of 5 kWh, enable the system to achieve around 80% self-sufficiency and self-consumption.

Alarmouty, T. et al. (2020) [24] applied a geothermal energy system in two different locations: an office building in Germany, where it was used for both heating and cooling, and at the American University of Madaba in Jordan. Applying this active strategy showed that a power system at a depth of 20 m is suitable for meeting the energy demands for a medium size residential building. The results showed a 60% reduction in energy consumption.

Hu, X. et al. (2021) [25] applied retrofit strategies to a one-storey dwelling with a gross area of 126.2 m^2 located in Jining, China aiming to improve indoor comfort and energy efficiency. A crystalline silicon PV system was installed on the pitched roof to supplement the building’s power demand needs and different thermal materials were used, such as Expanded Polystyrene EPS and rock wool insulation with varying thicknesses in each case to improve the thermal performance of the external walls. Applying retrofit strategies resulted in a reduction of energy use by 20.5%.

Ali, M. et al. (2023) [26] carried out the Installation of small-scale VAWTs on a building roof in Tabuk, Saudi Arabia and focusing on the H-Darrieus type, with NACA 0018 selected as the airfoil for the turbine blades (three blades with a chord length of 1 m and a diameter of 0.72 m) due to its ability to resist changes in the wind speed and angle of attack as shown in (Figure 2.3). ANSYS Fluent software was used as the simulation tool. A 2-D face mesh was applied, with 15,000 elements chosen as the fine mesh resolution. This simulation was executed at a wind speed of 10 m/s to align with the maximum experimental air velocity with a semicircular domain set to 12 times the chord length of the airfoil. The three-blade H-Darrieus VAWT can produce power at 3 m/s minimum wind speed, obtaining its rated power at 9 m/s. The maximum power coefficient obtained was 0.45 at a tip speed ratio of 1.94.

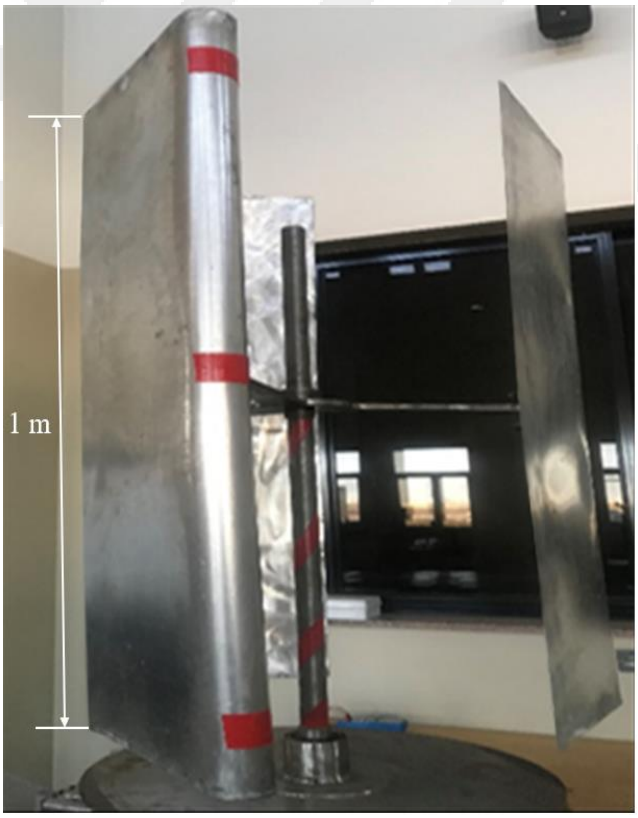

Figure 2.3 Three-Blade H-Darrieus Vertical Axis Wind Turbine [26]

Naik, K. et al. (2024) [27] used a type of Vertical Axis Wind Turbine (QR6 Helical Model) and Photovoltaic energy for attaining zero-energy home status instead of using costly passive retrofits. This study was conducted at the REMOURBAN PROJECT, Nottingham, UK. The study utilized two different methods to calculate the energy generation of the QR6 VAWT: the DesignBuilder simulation software and a Python program. The simulation recommended that VAWT energy output remained steady throughout the year. On the other hand, PV energy can produce sufficient power throughout the year. According to this research, although investment is required, the substantial energy generated by integrating a pair of QR6 Helical VAWTs was enough to consider 27 homes as zero-energy.

Ibrahim, A. et al. (2022) [28] experimentally conducted a hybrid small-scale VAWT, which combines Savonius and Darrieus rotors mounted on a gabled roof building which is considered suitable for the integration of hybrid-VAWT. The Savonius rotor had a height of 0.34 m, a diameter of 0.27 m, and a swept area of 0.0918 m^2, while the Darrieus rotor had a height of 0.4 m, a diameter of 0.35 m, and a swept area of 0.14 m^2. The prototype building has a gabled roof shape, and a building height of 0.7 m. Industrial fans were used as the wind source and the average wind speed was 5.8 m/s. The hybrid small-scale VAWT generated an output power of about 1.4 W without the building. When integrating onto the gabled roof shape, the power output increased close to 2 W under the same conditions. The hybrid VAWT achieved 20% of the rated power when the bare-hybrid VAWT generated only 14% of the rated power. additionally, the rotational speed (RPM) increased by 12% when mounted on the building rooftop.

Afify, R. (2019) [29] experimentally investigated and compared the performance of the IceWind with Savonius VAWT, considering aspects such as blade arc angle, aspect ratio, and number of blades. As shown in (Figure 2.4), the diameter of the IceWind blade was 75 mm with the height of 75 mm plus 25 mm blade tip height, the blade arc angle (ψ) was 112° and swept area was 4250 mm^2. These blades are made from Aluminium sheets. The IceWind turbine with triple, double, and reversed double blades was tested at five different speeds (8.4, 9.4, 11.5, 13.7, and 15.8 m/s) in a wind tunnel. With the same swept area, the IceWind turbine showed better performance than the Savonius wind turbine. In terms of rotational speed and static torque coefficients, the three-blade rotor exceeded two-blade and reversed double-blade rotors. Additionally, the blade arc angle ψ of 112° outperformed 135°. An aspect ratio (AR) of 0.38 with ψ= 112°, resulted in superior performance compared to the others in the study.

Figure 2.4 Three-Blade IceWind Turbine [29]

Suffer, K., and Jabar, Z. (2021) [30] numerically concluded a combined Hybrid IceWind-Darrieus vertical axis wind turbine (VAWT) as shown in (Figure 2.5) to solve the issue of low output torque by integrating IceWind blades with Darrieus design. The Darrieus airfoil had a height of 250 mm, a chord length of 83.33 mm, and a thickness of 14.16 mm. The dimensions of the IceWind blade had a of height 125 mm, a blade arc angle of 112.5°, and a thickness of 1.5 mm. The inlet velocity was considered as 10 m/s. The outcomes showed that the maximum drag coefficient (Cd) was 2.348 at a 120° blade angular position, while the minimum Cd was 1.527 at 0°. Static pressure drops and starting torque increased on the positive side and diminished on the negative side of the turbine rotor, thus the output power of the turbine increased.

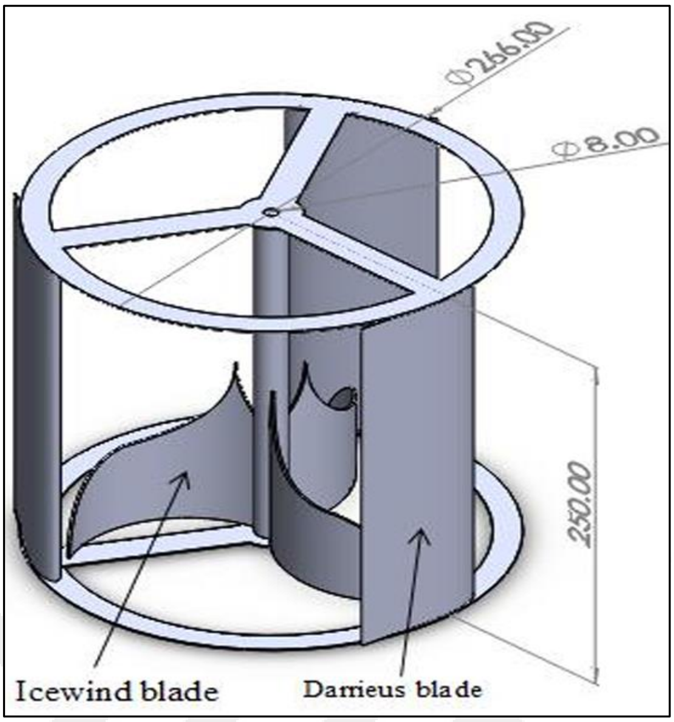

Figure 2.5 Hybrid Three-Blade IceWind-Darrieus VAWT [30]

Mansour, H., and Afify, R. (2020) [31] numerically compared a two-blade IceWind VAWT with the same blade dimensions as in the previous study [29], and a Savonius wind turbine. The 3-D ANSYS Fluent software was used to perform the simulation, with domain dimensions of the width, height, upstream, and downstream: 300, 300, 500, and 500 mm, respectively. The left boundary was set as a velocity inlet at 15.8 m/s, and the right boundary as a pressure outlet. Other boundaries and the IceWind turbine were considered as walls. A Mesh size of 7.8 x 10^{-6} cells was used with two zones: one rotating around the IceWind turbine and the other stationary. The Shear Stress Transport (SST) k-ω model, second-order discretization, and steady laminar flow were applied. The results showed similar patterns, but slightly lower values compared to the experimental results found in previous work. The vortices behind the IceWind turbine are larger compared to Savonius turbine, which caused to better energy capture and overall performance.

Al-Bahadly, I. (2009) [32] investigated a small-scale Savonius vertical axis wind turbine in rural buildings with detailed dimensions (0.65 m diameter and 1.5 m height). The main emphasis was on identifying a proper turbine that is basic and valuable. Tests were studied on the turbine rotor to measure operational speed under rated conditions to establish a gearing ratio using a pulley-V-belt configuration for optimal energy transfer to the generator, ensuring suitability for workshop and ease of storage or relocation (Figure 2.6). The Savonius rotor VAWT was considered an effective and feasible solution for specific small-scale electricity generation requirements, contributing a valuable foundation for further exploration and application in practical situations. The Savonius VAWT has many advantages despite its comparatively low efficiency such as its ease of design and construction.

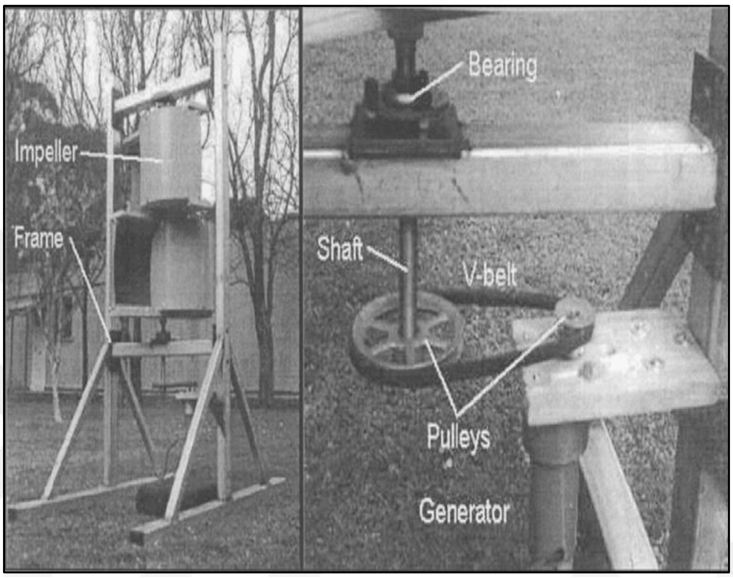

Figure 2.6 Complete Prototype Savonius VAWT Model [32]

Bahaj, A. et al. (2007) [33] discussed numerically the importance of small wind turbines within the building environment in the UK. A micro-wind tool was developed precisely for studying both energy production and payback periods. This tool is composed of four modules including energy usage, turbine performance, wind resource and carbon savings analysis. This analysis constituted the first step in assessing the suitability of using small wind devices in British residential buildings. A 400 W small-scale wind turbine was used in two different buildings heights in Aberdeen. The first building was at an altitude of 20 m, while the second building had a height of 10 m. (Figure 2.7) shows the wind speed and power output for these cases. It provided an accurate estimate of how much energy is likely to be exported from a given location and allows for more suitable financial calculations to evaluate the capital payback period (such as energy cost saving) for micro-wind turbines. if this capital payback period exceeded the life expectancy of the equipment, it becomes clear that the power generated by small wind turbines might not be financially viable. High rise buildings in urban environments are considered more suitable for installing micro wind turbines. Furthermore, micro wind turbines may be unsuitable for use in urban areas, due to turbulence and shadow effects which can reduce energy production by up to 50%. In contrast, rural and suburban sites, where open spaces and low objects reduce their effect on wind speed at typical rotor heights, are more suitable for installing small wind turbines.

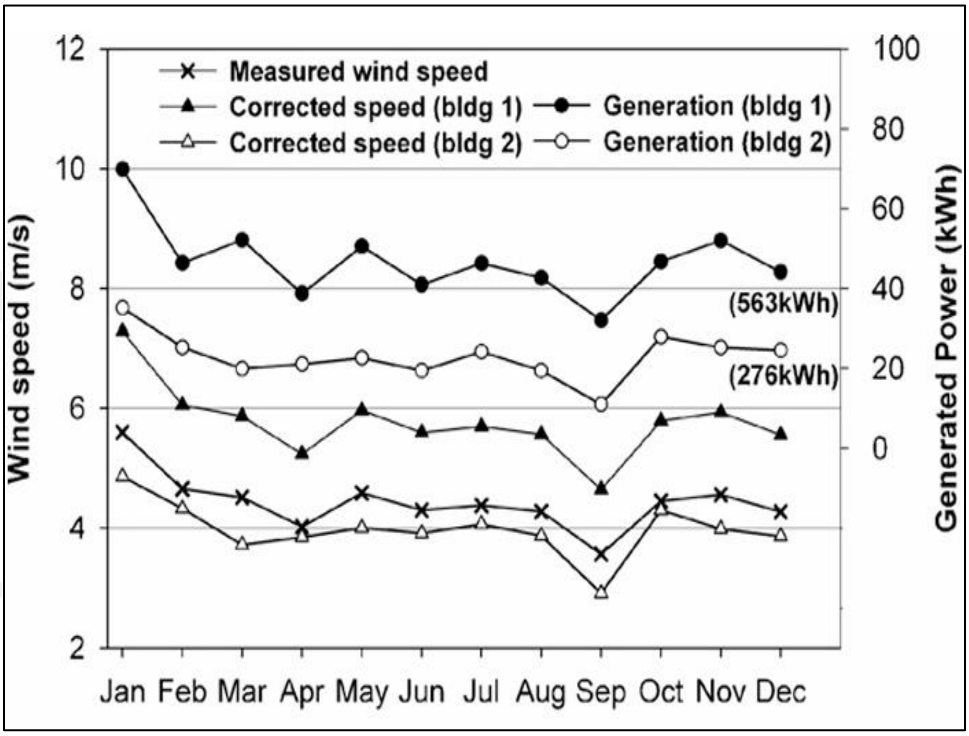

Figure 2.7 Wind Speed and Simulated Power Output on Two Building [33]

Turhan, C., and Saleh, Y. (2024) [34] investigated the integration of Ice-type vertical axis wind turbines (VAWTs) to reduce building energy consumption. The authors designed a three-blade IceWind with a 112° arc angle and an aspect ratio of 0.38. The rotor diameter was 2.2 m, with a swept area of around 1 m^2. The turbines were modelled using DesignBuilder Software to simulate energy performance. A small, two-storey building for soldiers on guard duty in Istanbul Airport, Türkiye, with an average wind speed of 4.9 m/s. A total of forty IceWind turbines were installed on the rooftop. These turbines were positioned in 10 circular columns, each column containing four turbines to ensure minimal aerodynamic interference. The power output for each turbine calculated as 72 W. The total energy savings around 9.3%, reducing annual energy consumption from 175.45 to 157.3 kWh/m^2.

Suffer, K., and Saleh, Y. (2024) [35] conducted the aerodynamic performance of IceWind VAWT blades using experimental and numerical methods. Two models were investigated, (model 1) with a blade height of 250 mm and another with 125 mm (model 2). The researchers fabricated models using 3D printing with Polylactic Acid (PLA) and measured in a low-speed wind tunnel at the University of Baghdad. ANSYS Fluent Software was used to conduct numerical simulation, applying the finite volume method and Shear Stress Transport SST k-ω turbulence model. Experimental results showed that (model 1) has a higher rotational speed of 610 RPM and a power coefficient 0.0688 compared to (Model 2), which has a rotational speed of 265 RPM and a power coefficient of 0.03551. numerical results confirmed that (model 1) with a maximum static pressure of 69.39 Pa and a maximum velocity of 13.5 m/s, exceeding (model 2) in all aspects.

Saleh, Y. et al. (2024) [36] analyzed energy-efficient reconstruction methods, including IceWind VAWTs, thin-film photovoltaic (PV) panels, and green walls. A five-storey residential building in Kurtlusarımazı, Hatay, Türkiye, with a total floor area of 424 m^2. The study used Shear Stress Transport (SST) k-ω turbulence model for aerodynamic performance evaluation of the Vertical Axis Wind Turbines VAWTs. A tetrahedral mesh was applied for CFD simulation and DesignBuilder Software was utilized for building energy simulation. Each turbine was designed with a diameter of 0.7575 m, height of 1.456 m. The 42 IceWind turbines were installed on the rooftop of the building. Hedera Canariensis Gomera was used for insulation, reducing cooling energy. Using thin-film PV panels increased by up to 20% due to bifacial design. The baseline building's energy demand was 182.4 kWh/m^2 annually. The authors pointed out that the integration of IceWind turbines reduced energy use by 8.5%, PV panels decreased consumption by 18%, while green walls observed a 4.1 reduction. Combined strategies resulted in a 28.5% energy savings with a payback period of 7.4 years.

Saleh, Y. et al. (2024) [37] examined the integration of small-scale VAWTs in dwelling units. The research focused on two types: Savonius and IceWind turbines. The study was conducted in Karaburun, İzmir, Türkiye with wind speeds varying between 6 and 8 m/s. building includes three storeys with a total floor area of 397 m^2, and the U-value of external walls was found to be 0.317 W/m^2K. DesignBuilder and ANSYS Fluent were conducted using the Shear Stress Transport SST k-ω turbulence model. The IceWind had a diameter of 0.7575 m and height of 1.456 m. The IceWind turbine reduced the building's energy consumption by 22.5%. The Savonius type, with a diameter of 1.515 m and swept area of 2.28 m^2, resulted in a 36% decrease in energy consumption. The IceWind turbine had a payback period of 14.57 years. In contrast, the Savonius turbine had a shorter payback period of 8.93 years, making it the more economically sustainable option. (Figure 2.8) shows the Savonius turbines mounted on the rooftop of the building. The Savonius turbine achieved better efficiency due to its higher power output 502 W compared to the IceWind turbine 305 W.

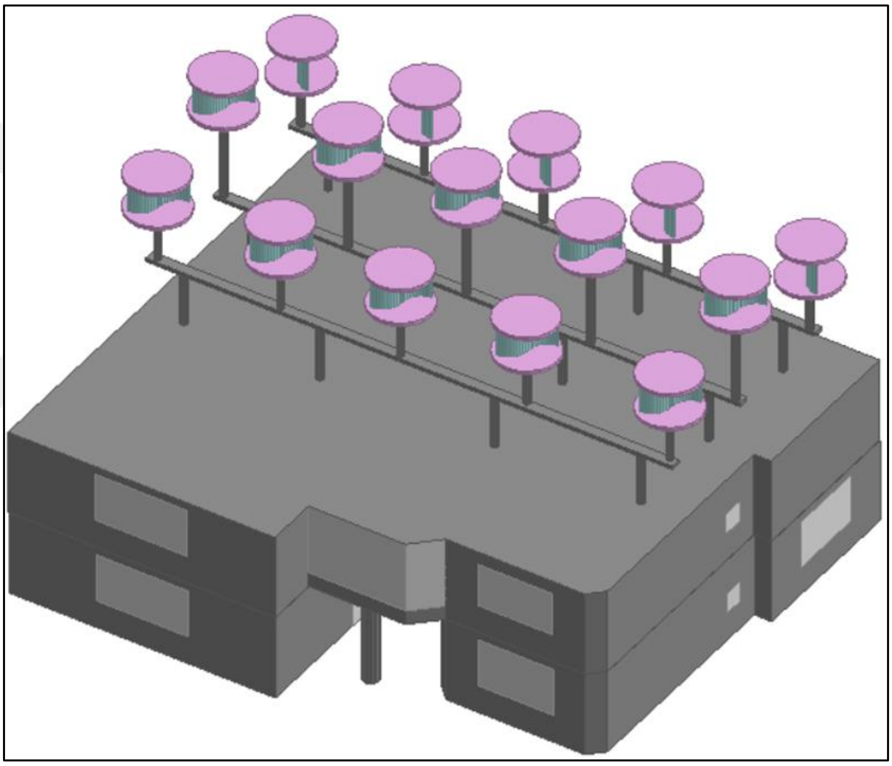

Figure 2.8 Savonius Turbines Mounted on the Building [37]

Chong, W. et al. (2017) [38] developed a new Cross Axis Wind Turbine (CAWT) designed for urban environment. This turbine includes six horizontal blades and three vertical blades. The novel compared the CAWT with straight-blade VAWT to evaluate efficiency improvements. This study was conducted on a building with a gable roof at the University of Malaya, Malaysia. The authors used both experimental and numerical simulation to analyze the turbine's efficiency. For the simulation, the researchers applied the Shear Stress Transport SST k-ω turbulence model in ANSYS Fluent software. The results showed that the CAWT achieved a maximum power coefficient Cp of 0.1263 at a Tip Speed Ratio TSR of 1.1, which was measured to be 266% greater than the VAWT at the same height. The study revelated that wind speed increased by 19% to 33% due to the rooftop acceleration effect. The combination of experimental testing and numerical simulation confirms that the CAWT can be a viable strategy in context of building-integrated wind energy systems.

Kavade, R., and Ghanegaonkar, P. (2022) [39] examined a small-scale VAWT with a variable pitch mechanism to enhance power output. The turbine incorporates a Darrieus-type design with a NACA 0018 airfoil with a blade height of 600 mm and a diameter of 600 mm. The turbine with four blades utilizes a cam and follower mechanism for pitch control and was experimentally tested in a controlled wind environment using an axial fan-generated wind flow. The authors validated the results using a MATLAB-based computational approach. A maximum power coefficient Cp of 0.35 was observed at a Tip Speed Ratio TSR of 2.5 and a wind speed of 10 m/s. The research indicated that this variable pitch VAWT is suitable for residential buildings in urban environment with consistent wind flow.

Ali, N. et al. (2019) [40] discussed six different models of Darrieus VAWTs. The airfoil profile used in all models is DU06W200, which was developed at Delft University of Technology. Three types of blade designs were tested: Straight blades, twisted blade (70°), and Helical blades (120°), each design was examined with two and three blades' configurations. The turbines were fabricated using a 3D printer with PLA material. The researchers carried out both experimental wind tunnel tests and numerical simulations using ANSYS CFX. The experimental setup included a wind tunnel with airflow speed between 3 and 7.65 m/s. The numerical analysis used the SST k-ω turbulence model to validate the experimental findings. Prismatic mesh applied near the blades to capture boundary layers accurately. The two-bladed Straight-type achieved the highest efficiency, with a power coefficient Cp of 0.2495 and a rotational speed of 198 RPM at a wind speed of 3 m/s. In contrast, helical designs required at least 5 to 6 m/s to start rotation, making them less effective under low-wind conditions.

Redchyts, D. et al. (2023) [41] explored the aerodynamic performance of Savonius and Darrieus VAWTs using Computational Fluid Dynamic (CFD). The effects of tip-speed ratio, Reynolds number, and solidity on turbine efficiency were evaluated. The study used Reynolds-Average Navier-Stokes (RANS) equations to simulate the flow around the rotors. The computational setup employed structured grids, with 600,000 nodes for the Darrieus VAWT and one million nodes for Savonius VAWT. Numerical tests were performed on three and two blades Savonius rotor designs, with the two-blade rotor achieving a maximum power coefficient od 0.23, while the three-blade rotor reached to 0.19. The study analyzed single-blade, two-blade, and three-blade rotor setups of the Darrieus-type. The results indicated that the power coefficient increased from 0.15 to 0.5 as the number of Reynolds rose from 104 to 106. Additionally, the researchers observed that a lower solidity (from 1.0 to 0.33) reduced the effect of the tip-speed ratio on performance. Consequently, the findings showed that the Darrieus-type achieved higher efficiency, whereas the Savonius-type provided more stable performance.

Divakaran, U. et al. (2021) [42] compared three helical-bladed VAWT designs with angles of 60°, 90°, and 120°, using ANSYS Fluent Software. The turbine included a 1 m diameter and a 3 m height. The NACA 0015 airfoil was used for the blade profile and the chord length of each blade is 210 mm with a solidity of 0.4. The study employed the Transition SST k-ω turbulence model. A mesh independence analysis was conducted using 21, 14, and 9 million grid points. Results suggested that the 60° helix angle achieved the highest efficiency, particularly at a TSR of 3.3. Furthermore, the study showed that helix angles improved wake dissipation, which is perfect for placing multiple turbines close proximity. The 60° configuration demonstrated the best power output, while the 120° design reduced mechanical stress. The findings supported the further development of helical VAWTs for urban wind energy applications. (Figure 2.9) presents the effect of various helical angles on the coefficient of performance of the VAWT.

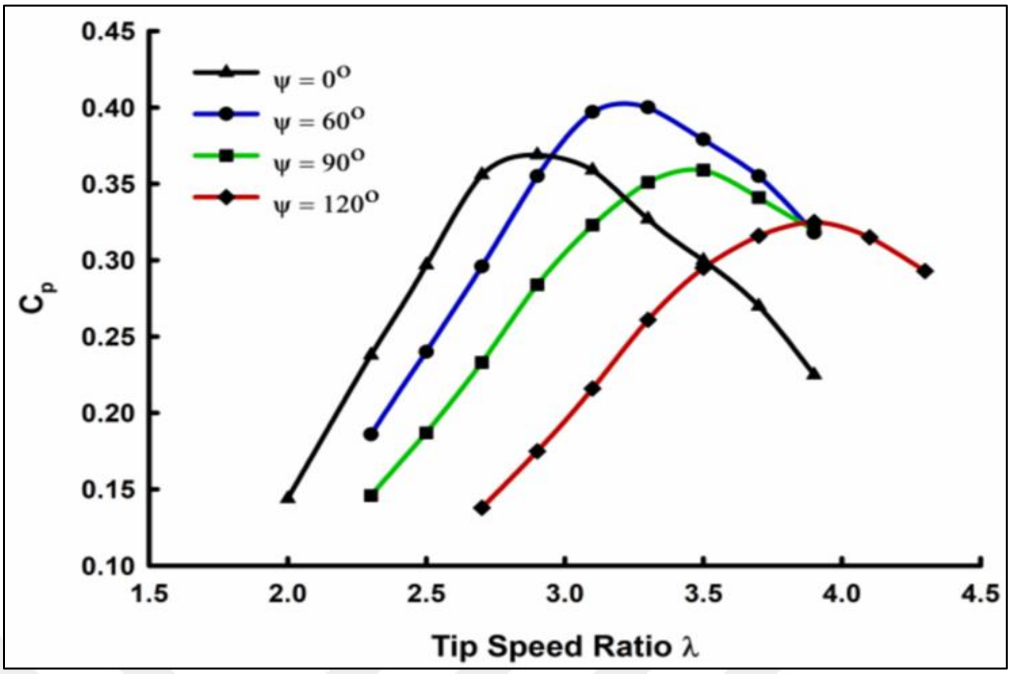

Figure 2.9 Impact of Helical Angles on the Performance of VAWT [42]

Issac, L. et al. (2022) [43] examined the design and performance of a Helical Cross Axis Wind Turbine (HCAWT) for urban applications. The HCAWT consists of three helical vertical blades and six horizontal blades placed together. The rotor had a diameter of 350 mm, a horizontal blade length of 150 mm, and a vertical blade height of 300 mm. The Computational Fluid Dynamic CFD simulation was performed using SimScale Software. The SST k-ω turbulence model was applied, and a steady-state simulation was conducted using the SIMPLE algorithm. The results demonstrated that HCAWT achieved a maximum power coefficient Cp of 0.52 at Tip Speede Ratio TSR of 1.61 but the straight-bladed VAWT reached a maximum Cp of 0.32 at TSR of 0.66. The authors emphasized that HCAWT can be installed on various building rooftops and offered better efficiency.

Suresh, A. et al. (2023) [44] assessed the performance of helical VAWTs using Aluminium-based. Two airfoil profiles, NACA 0012 and NACA 0018, were studied to verify their effectiveness in helical blade configurations. SolidWorks software was employed to create 3D models of turbine blades and CFD simulation of velocity and pressure contours at wind speed of 5 and 10 m/s were conducted using ANSYS Fluent Software. The results showed that NACA 0018 generated higher drag, making it more suitable for helical VAWTs. Alternatively, NACA 0012 had a higher lift and drag ratio, making it efficient for scenarios where high lift is required. Furthermore, the study carried out 2D flow analysis and calculated power and torque using ANSYS CFX software. The power output was 1.2 W, while the mean torque was 0.01 N.m. The authors suggested that future work should include analysis of different blade designs.

Han, D. et al. (2018) [45] carried out a 100-W helical VAWT developed for urban applications. The turbine's profile was NACA 0018, and it had four blades with a chord length of 0.25 m. The rotor height and radius were 1.43 m and 0.55 m, respectively, resulting in a swept area of 1.57 m^2. The turbine's power output was estimated using a momentum-based design method under IEC 61400-2 standards. For numerical analysis, 2D CFD simulations were conducted to analyze the lift and drag coefficients at different angles of attack. The SST k-ω turbulence model was used in Unsteady Reynolds-Averaged Navier-Stokes (URANS) analyses. A grid system with 575,142 elements and 1,162,500 nodes was used to capture detailed flow characteristics. A mathematical model predicted power output as 108 W, while wind tunnel experiments measured 114 W. the power coefficient Cp at 9 m/s and 170 RPM was 0.163. The results confirmed that the mathematical model predicted turbine performance it high accuracy, making it a valuable tool for designing low-speed, urban wind turbines.

Mohammed, G. et al. (2021) [46] examined a hybrid VAWT integrating Darrieus and Savonius rotors for rooftop applications. The study aimed to improve wind energy by combining the self-starting ability of Savonius rotor with the high efficiency of Darrieus rotor. The hybrid turbine featured a double-stage Savonius rotor with three Darrieus blades. The Savonius rotor had a 0.27 m diameter, while the Darrieus rotor had a 0.35 m diameter. The results indicated that building integration significantly enhanced turbine performance. The rotational speed increased by 33% compared to a bare-hybrid VAWT. The mechanical power output of the building integrated hybrid VAWT rose by 55%. The rooftop acted as a wind accelerator, enhancing efficiency due to the speed-up effect.

Gad, T. et al. (2020) [47] carried out the performance of IceWind turbines with different blade configurations. The study evaluated two-blade, three-blade, two-reversed blade, and four-blade designs in a wind tunnel. The turbine rotors were made from stainless steel, and their dimensions were 200 mm rotor height and 117 mm rotor diameter. The analysis showed that the three-blade IceWind Vertical Axis Wind Turbine VAWT had the highest static torque and rotational speed, making it the most effective design. In contrast, the four-blade design had the lowest performance.

Lillahulhaq, Z. et al. (2021) [48] conducted the effectiveness of IceWind and Savonius Vertical Axis Wind Turbines VAWTs. A fan was used to simulate three-blade designs for both types. The results contradicted previous studies, which tested IceWind turbines with different aspect ratios. The result showed that IceWind-type generated higher static torque. The Savonius-type had a higher power coefficient CP and efficiency. The IceWind turbine operated efficiently at a tip speed ratio TSR between 0.5 to 0.8. in contrast, Savonius-type delivered the highest efficiency with a TSR range of 0.65 to 0.85.

Zheng, M. et al. (2016) [49] studied the effect of increasing the number of blades for a Vertical Axis Wind Turbine VAWT and its correlation with turbine efficiency. Three different designs of VAWTs with 3, 5, and 6 blades were investigated using numerical analysis with the wind speed fixed at 8 m/s. The results showed that using three-blade VAWT could generate an efficiency of 20.44% at 20 RPM. Utilizing five-blade results in an efficiency of 24.3% at 17 RPM. The highest efficiency of 26.82% at 18 RPM was achieved with a six-blade turbine. The study demonstrated that the average torque value for the three-blade turbine was 199.79 N.m. Conversely, employing 5 and 6 blades, the average torque values were found to be 279.69 and 291.44 N.m respectively. The researchers suggested that the values should be adopted for the design of VAWTs and to obtain the optimum dimensions with the number of blades.

Karadag, I., and Yuksek, I. (2020) [50] reviewed the use of horizontal and vertical wind turbines in various buildings worldwide. Three Horizontal Axis Wind Turbines HAWTs with a diameter of 29 m were used in the Bahrain World Trade Centre. The turbines were placed in the centre of the building towards the wind, which made the wind capture rate reach 30%. In the Pearl River Tower, which is 309 m high, four Vertical Axis Wind Turbines VAWTs are installed. Each turbine has 8 m high and operates efficiently within a range of 27-40 m/s. The rated power of each one was 8 kW. Overall, the researchers pointed out the importance of analyzing long-term climate data.

Table 2.1 Summary of Reviewed Studies on Vertical Axis Wind Turbines VAWTs

Authors	Year	VAWT Model Used	Number of Blades	Diameter of Wind Turbine (m)	Purpose
Ali et al. [26]	2023	H-Darrieus (NACA 0018)	3	0.72	Testing rooftop wind perofrmance
Naik et al. [27]	2024	QR6 helical	3	Not specified	Achieving net-zero in 27 homes
Ibrahim et al. [28]	2022	Hybrid	3 (Darrieus) + 2-stage (Savonius)	0.35 (Darrieus) , 0.27 (Savonius)	Improving rooftop turbine efficiency
Afify [29]	2019	IceWind	3	0.075	Evaluating IceWind turbine performance experimentally
Suffer et al. [30]	2021	Hybrid	6	Not specified	Improving starting torque of Darrieus type
Mansour et al. [31]	2020	IceWind	2	0.075	Studying 3D flow over IceWind turbine
Al-Bahadly [32]	2009	Savonius	2	0.65	Providing power for rural homes
Turhan and Saleh [34]	2024	IceWind	3	2.2	Reducing energy use in Istanbul building
Suffer and Saleh [35]	2024	IceWind	3	Not specified	Comparing two IceWind desgins in CFD and experimental
Saleh et al. [36]	2024	IceWind	3	0.7575	Reducing energy use in post-earthquake housing
Saleh et al. [37]	2024	IceWind and Savonius	3, 2	1.515, 1.515	Comparing payback and energy savings
Kavade and Ghanegaonkar [39]	2022	Darrieus (NACA 0018)	4	0.6	Improving Cp using variable pitch control

Table 2.1 (continued)

Aljabair et al. [40]	2019	Darrieus (DU06W200)	2, 3	0.5	Comparing 6 models at low wind speed
Redchyts et al. [41]	2023	Darrieus and Savonius	2 , 3	0.5	Studying unsteady flow and power coefficient
Divakaran et al. [42]	2021	Helical	3	1	Studying the effect of helix angle on performance
Suresh et al. [44]	2023	Helical	3	0.2	Analyzing airfoil impact and structural stability
Han et al. [45]	2018	Helical	4	1.1	Designing and testing a 100W turbine at low TSR
Gad et al. [47]	2020	IceWind	2, 3, 4	0.117	Finding the optimal IceWind blade number experimentally
Lillahulhaq et al. [48]	2021	IceWind and Savonius	3	0.345	Comparing the perofrmance of IceWind and Savonius

This study differs from previous studies by focusing on a comprehensive simulation of turbine performance and applying it on a realistic residential building in İzmir, Türkiye. Most previous studies focused solely on aerodynamic analysis or investigated only a single turbine type, such as the Helical or Savonius Vertical Axis Wind Turbine VAWT. This study simulated three types of VAWTs and proposed a new design using three IceWind blades paired with three helical blades bent at 60°, a design that has not been covered in previous studies. The closest work was by Suffer and Jabar [30], who analyzed IceWind and Straight-blade Helical VAWTs but without looking at how they affect energy use or applying them to an actual residential building.

Therefore, the aim of this thesis to design three novel small-scale wind turbines and compare their energy cosumption potentials. The novelty of this thesis is to show the importance of small-scale wind turbines applied to the top of the buildings. In addition, the placement of the wind turbines is new for the literature.

CHAPTER 3

METHODOLOGY

In this chapter, the details of the study process are explained. Three different types of Vertical Axis Wind Turbines VAWTs were applied. They were simulated on the roof of a residential building in İzmir, Türkiye. The aim of placing these turbines is to reduce the energy consumption in the building. In addition to making the most of the environmentally friendly wind energy. The effect of each of the three types used in this study was compared and analyzed. Their effect varies under environmental conditions. Numerical analysis of these turbines helps to choose the most efficient and least cost type. (Figure 3.1) shows the flowchart of the work step by step, starting from designing the turbines, collecting data, and then obtaining and analyzing the results.

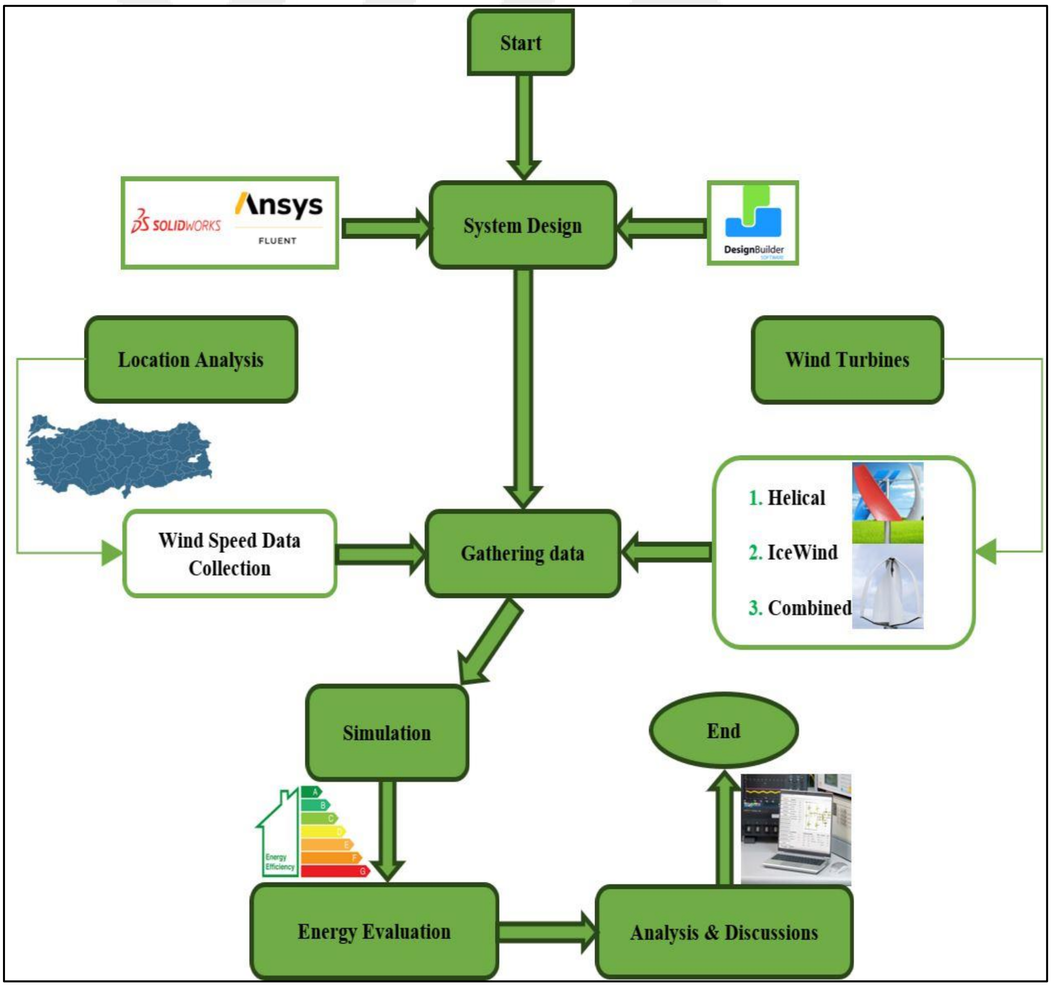

Figure 3.1 Flow Chart of the Study

3.1 Climate and Location Analysis

Türkiye has many areas with high average wind speeds and is suitable for vertical axis wind turbines VAWTs. It has been found that one of the best locations for installing wind turbines in urban areas is İzmir. İzmir is located at latitude 34.42° N and longitude 27.14° and is classified as a Mediterranean according to the Köppen Geiger classification [51]. It is a global climate classification that shows the effects of temperatures and rainfall rates in all regions of the world. Countries of the world are classified into five levels: temperate, arid, continental, tropical and polar climates. Each of them is distinguished by a specific colour to indicate the nature of the region and facilitate researchers' identification of the climate.

Izmir is distinguished by its strategic location and a population of 4.4 million people. This city has had national and regional importance for about a hundred years [52]. The recent increase in investments in the wind sector, especially in İzmir, has made it the focus of attention for many wind companies. The use of wind energy in these areas is an ideal solution to reduce energy consumption rates, which contributes to reducing the economic burden on the government [53].

Atlas is a site that shows the annual wind speed and specializes in studying the nature of winds in countries around the world [54]. After studying most areas in terms of average wind speed, it was found that one of the best locations for installing vertical wind turbines in the urban environment is in the Çeşme region of İzmir, Türkiye. The Çeşme region is characterized by an average annual wind speed of about 7 m/s. This makes it an ideal location for capturing wind and generating energy through small-scale vertical axis wind turbines.

(Figure 3.2) shows the average annual wind speed for the city of Izmir. The ideal location for installing vertical axis wind turbines is in Çeşme, located west of the city of İzmir. The red mark indicates the location of the building in the research study where the vertical axis wind turbines were installed and then analyzed to see the energy reduction rates.

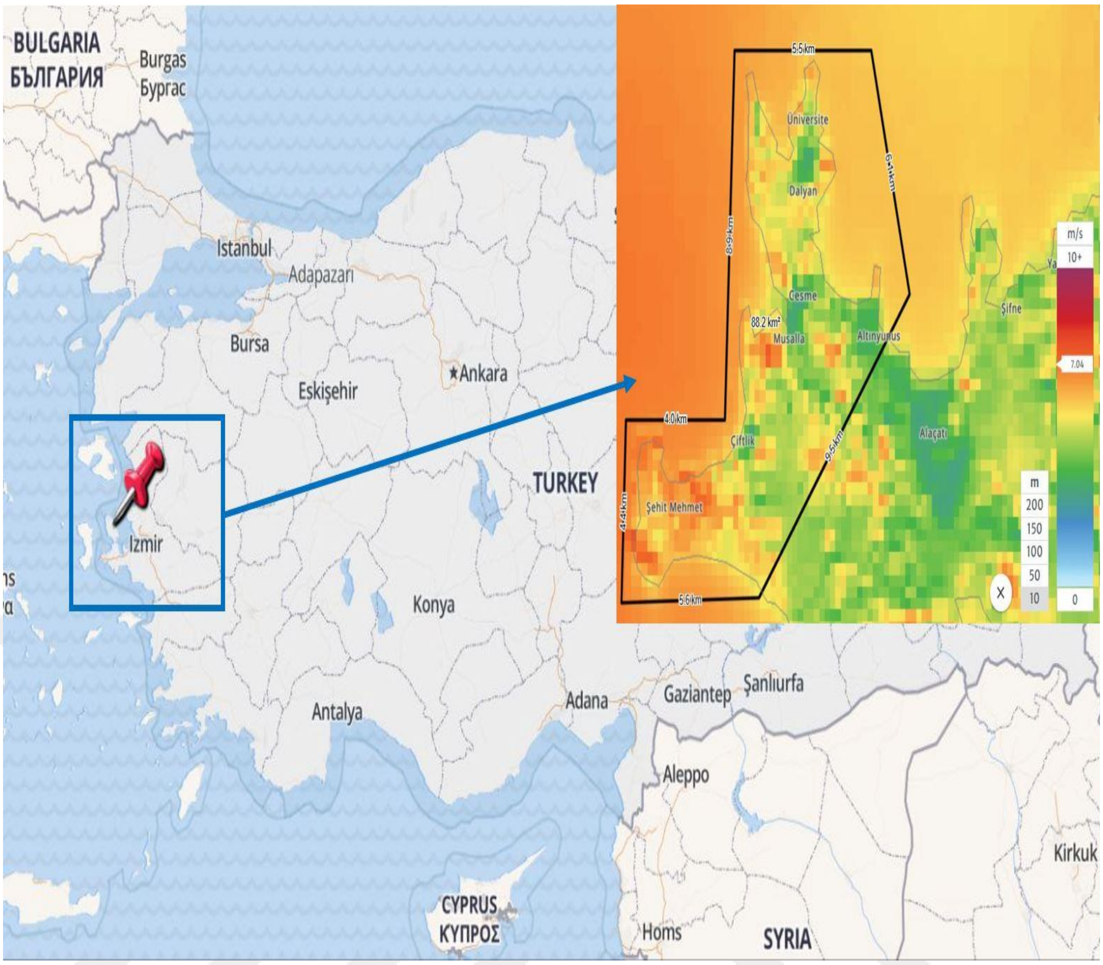

Figure 3.2 Location of Çeşme and Average Wind Speed

3.2 Case Building Design

The case building in Çeşme, İzmir, Türkiye is conducted as a case study and baseline design. The model building was used as a five-storey residential building. Each floor has two apartments. The total area of the building is 2120 m^2 and contains 115 parts. Each apartment consists of a guest lounge, a kitchen, a living room, three bedrooms and two bathrooms. In addition to other annexes such as a storeroom, two balconies and an entrance. This building was designed after a complete study of the Turkish Standard TS 825 [55]. The measurements of the existing doors and windows were taken into consideration, and they are in accordance with the municipal regulations of the Turkish government [56]. (Figure 3.3) shows the architectural drawing of the building.

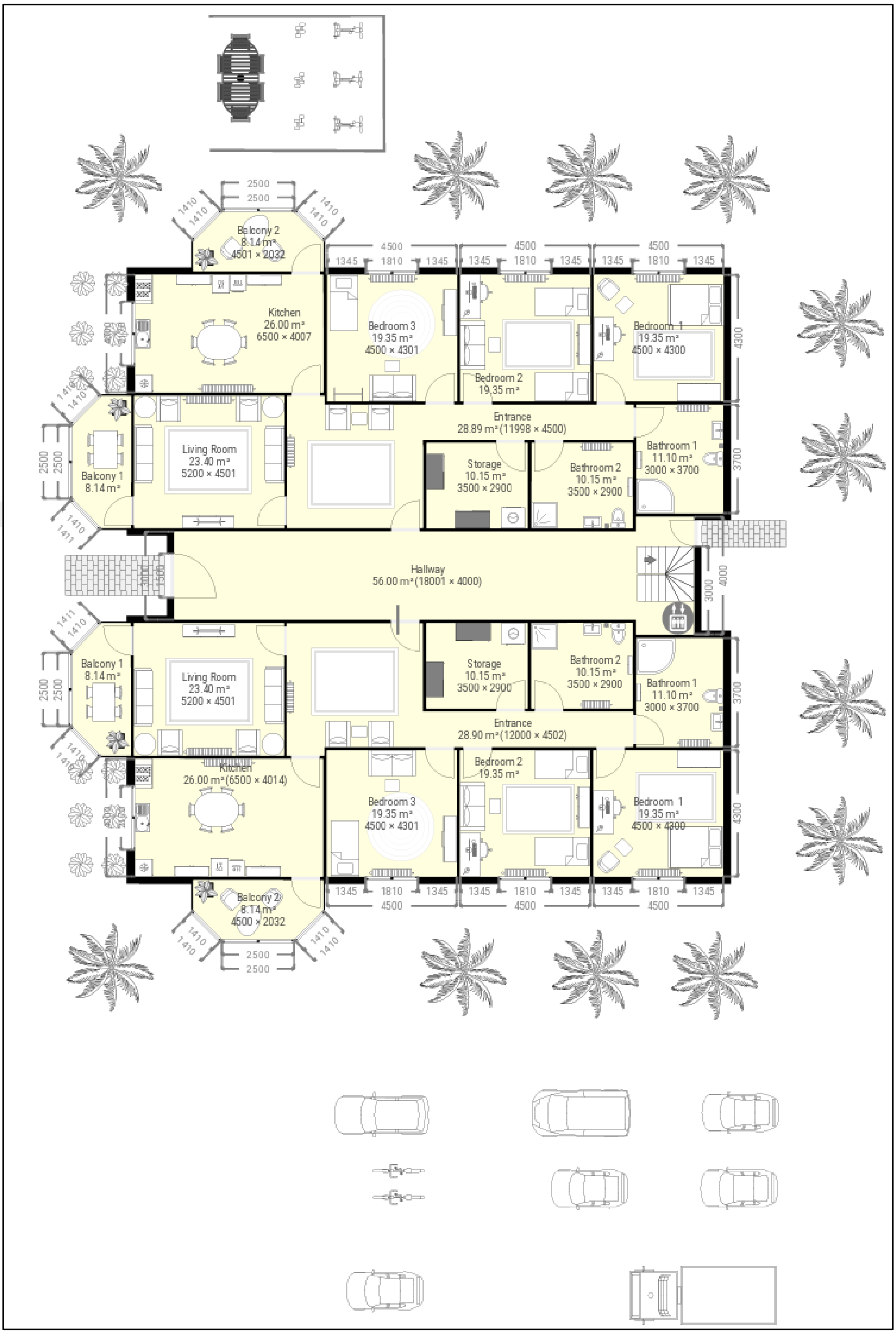

Figure 3.3 Architectural Drawings of the Residential Plan

The layers of building materials were used starting from the outer layer to the inner layer as shown in the table 3.1 below. The table shows the type of each material with its conductivity and thickness.

The external wall layers are composed of (cement sand render, expanded polystyrene (EPS), concrete block (Medium), expanded polystyrene (EPS), and gypsum insulating plaster). The flat roof layers consist of (gravel, bitumen felt, screed, polyurethane foam, and reinforced concrete). The ground layers are constituted by (carpet or textile, screed, reinforced concrete slab, polyurethane foam, sand and gravel).

Table 3.1 Building Envelope Layers and Thermal Properties

Construction Layers	**Thickness (m)**	**Thermal Conductivity (W/mK)**
External walls		
Cement sand render	0.015	1
Expanded polystyrene (EPS)	0.08	0.046
Concrete block (Medium)	0.25	0.51
Expanded polystyrene (EPS)	0.03	0.046
Gypsum insulating plaster	0.015	0.18
Roof		
Gravel	0.03	2
Bitumen felt	0.004	0.23
Screed	0.03	0.41
Polyurethane foam	0.08	0.028
Reinforced concrete	0.18	2.3
Ground		
Carpet or textile	0.015	0.06
Screed	0.05	0.41
Reinforced concrete slab	0.12	2.3
Polyurethane foam	0.07	0.028
Sand and gravel	0.21	2

By selecting the material for each layer and its thickness, the thermal transmittance values for all layers within the residential building can then be extracted, as shown in table 3.2, which shows all the values for the building with a complete summary of the building specifications and their components.

Table 3.2 Basic Design Features

Building Construction Properties	Values
Number of storeys	5
Number of spaces	115
Overall building area	2120 m^2
External walls (U-value)	0.317 (W/m^2K)
Internal walls (U-value)	1.923 (W/m^2K)
Roof (U-value)	0.314 (W/m^2K)
Ground floor (U-value)	0.309 (W/m^2K)
Glazing type + U-value	Reference glazing with 1.978 (W/m^2K)

3.3 Energy Simulation Analysis

DesignBuilder software was used in this study to design the building and then simulate the wind turbines on the roof of the building [57]. This software is important in the field of construction and energy consumption calculations in various types of buildings such as schools, hospitals, residential buildings, etc. The software contains all the weather data that is simulated during the building analysis. The software also provides complete calculations regarding the amount of energy consumption by using renewable energies such as wind energy or solar energy. İzmir weather database file (IZMIR-TUR IWEC) was used in this study. When this data was selected, automatic simulation of all weather conditions throughout the year in İzmir was conducted.

The architectural drawings map was entered into the Design Builder program in two-dimensional form. The architectural plan of the residential building was drawn. Each part within the architectural drawings is defined as zones. (Figure 3.4) shows the three-dimensional drawing of one floor from within the DesignBuilder software. All the building contents can be seen with a name given to each zone. After completing the drawing of the ground storey of the building, the windows and doors were placed with the appropriate measurements for each zone. All these initial stages come before entering into the construction layers for the external walls, internal walls, roof and ground.

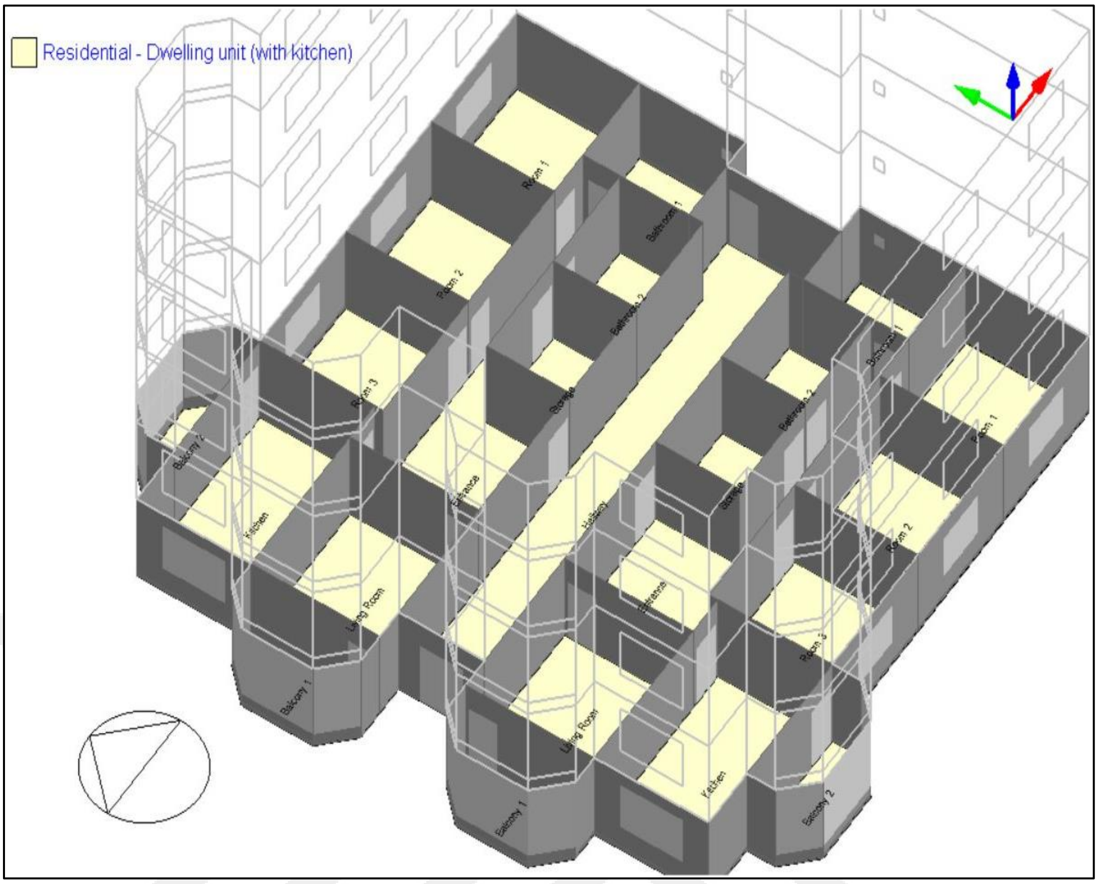

Figure 3.4 3D Shot of the Basic Design Model Inside the Building

After completing the ground storey of the case building, the clone command was used within the DesignBuilder software. This made it easy to complete the building drawings for the other storeys and made the building complete in detail. Each storey contains the same number of rooms, bathrooms and other parts. Mechanical ventilation was considered inside the bathrooms. In addition to calculating all the requirements for other electrical devices and setting their value within the software. These values were taken into consideration when conducting the annual analysis of electricity consumption within the residential building.

(Figure 3.5) shows the final design of the five-storey residential building. Windows and balconies are arranged in a way that ensures natural lighting and optimal ventilation. The building is square in shape and has a large area on the roof to install vertical wind turbines in a way that can capture wind from all directions. The final design reflects a modern vision that meets the residents' needs in terms of comfort and safety.

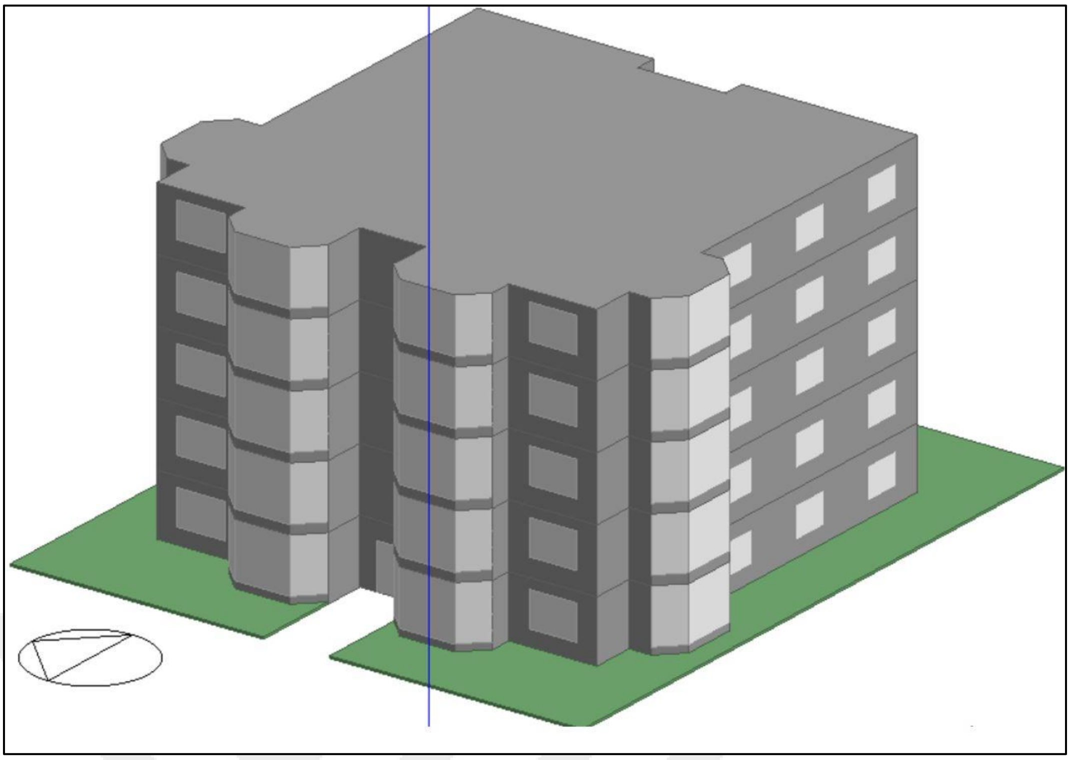

Figure 3.5 3D Shot of the Basic Design Model Outside the Building

(Figure 3.6) shows the dynamic analysis of the building and the sun's orbit throughout the year, in addition to the sunrise and sunset hours. This preliminary analysis is conducted to ensure that there is no problem in the building design before starting to use turbines on the roof of the building.

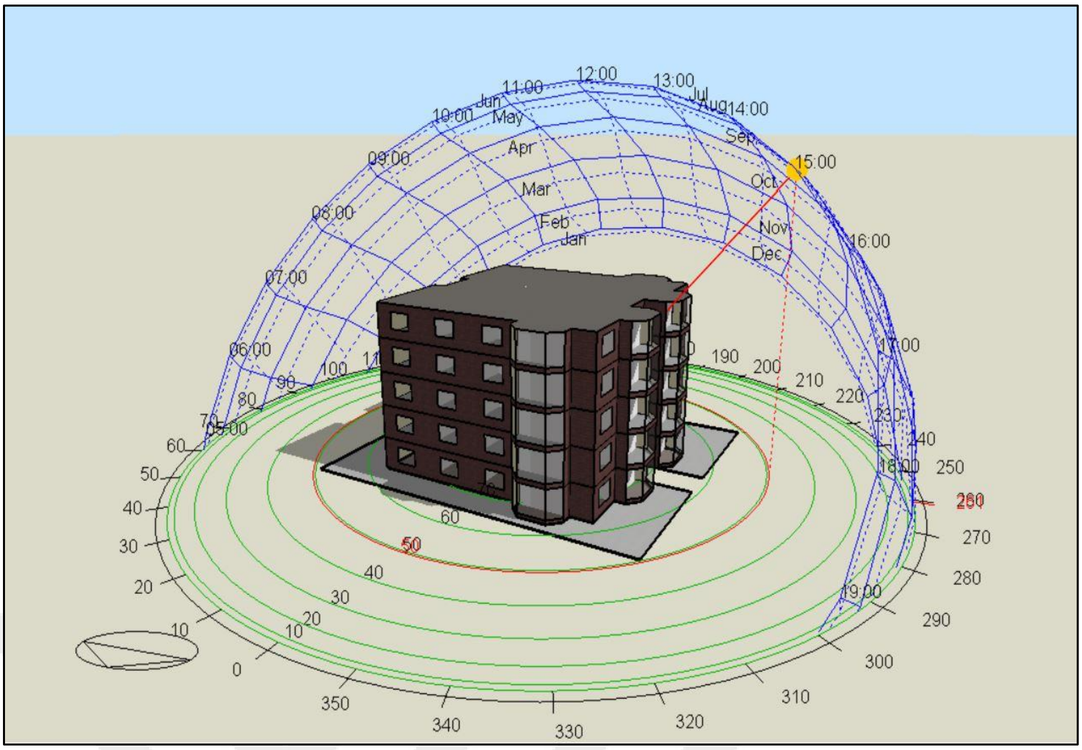

Figure 3.6 Energy Simulation Model of the Case Building

3.4 Retrofitting Strategies

Three different types of vertical axis wind turbines VAWTs were used. The first type includes a vertical axis IceWind turbine with three blades. The second type is a three-blade Helical type. The last type is an innovative design that combines the IceWind and Helical types with a total of six blades. The number of turbines used on the roof of a residential building, numerical analysis and the efficiency of the wind turbine in an urban environment were explained.

3.4.1 Case One (Case 1): Building-Integrated Ice-Wind Turbine

- **Ice-Wind Turbine Design**

IceWind vertical axis wind turbines VAWTs are characterized by their ability to rotate at low speeds. The turbines start rotating at 3 m/s. Their special blade type and curves make them suitable for use in cold and snowy regions.

SolidWorks software, a widely used software for designing 3D shapes, was used to design the turbine blades. The researcher can then perform simulation or numerical analysis according to the study objective [58].

The calculations for the vertical axis wind turbine dimensions were taken according to previous studies and the new dimensions were made according to the IEC 61400-2 regulation. These regulations are considered the reference for the design of small-scale wind turbines. This standard provides guidelines and technical specifications for the design of wind turbines. The factors adopted for the design of the turbine are efficiency, safety and reliability [59].

Table 3.3 shows the specifications of the IceWind turbine. The Ice-blades were designed to be thin sheet arranged at an arc angle of 112°.

Table 3.3 Parameter and Dimensions of the IceWind Rotor

Parameter	Value	Units
Diameter	1.515	m
Height	1.456	m
Swept area	1.950	m^2
Free stream velocity	7	m/s
Number of blades	3	-

(Figure 3.7) shows the final configuration of the IceWind turbine before numerical analysis.

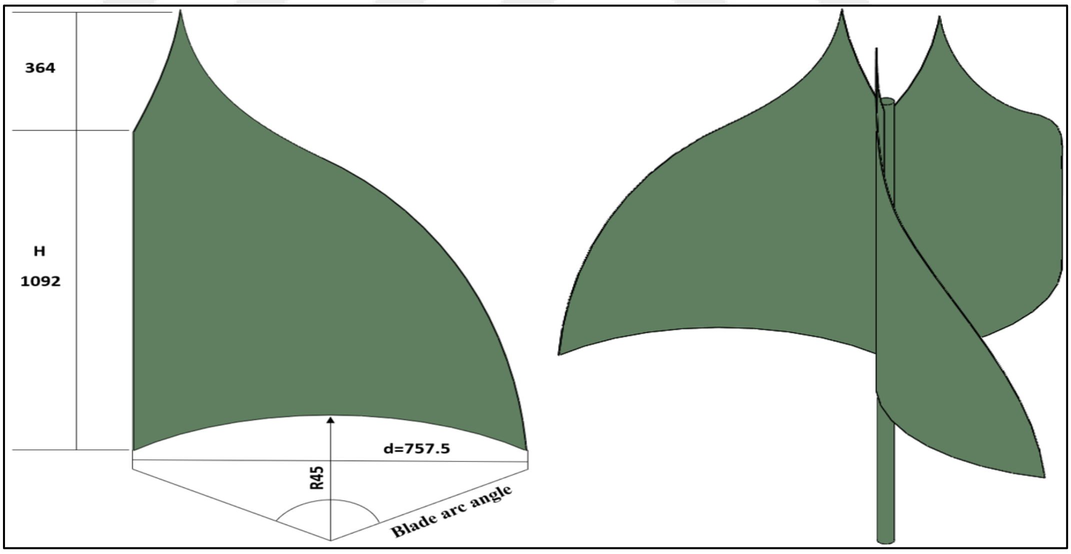

Figure 3.7 Ice-Wind Turbine Dimensions (All Units Are in mm)

- **Setting Computational Domain and Mesh Generation**

An ANSYS Fluent software is used as a numerical simulation tool for wind turbines, which is a special tool for performing numerical verification [60]. The software uses the finite element method to solve complex simulation problems. ANSYS Fluent is capable of handling various types of flows such as turbulent and laminar flows.

The process of obtaining the results of numerical analysis progresses through several stages, after entering the geometry of the turbine from an external file in Step file from the SolidWorks software inside the ANSYS Fluent. Then the second stage begins, concerning the domain, through which the required range for the simulation is determined. As for the last stage before starting the numerical analysis, it is the mesh, through which the accuracy of the results and the speed of the calculations are determined.

The dimensions are (6000 x 3000 x 3000) mm, and it has been considered in the Computational Fluid Dynamics computation. The domain was set as follows: the inlet velocity is set as 13 m/s, and no-slip boundary conditions on all the other surfaces. The pressure outlet is set to 0 pa gauge pressure, ensuring atmospheric exit conditions. The blades are modelled as rigid in simulation.

(Figure 3.8) shows all dimensions of the boundary conditions, in addition to the direction of the inflow wind and the location of the turbine.

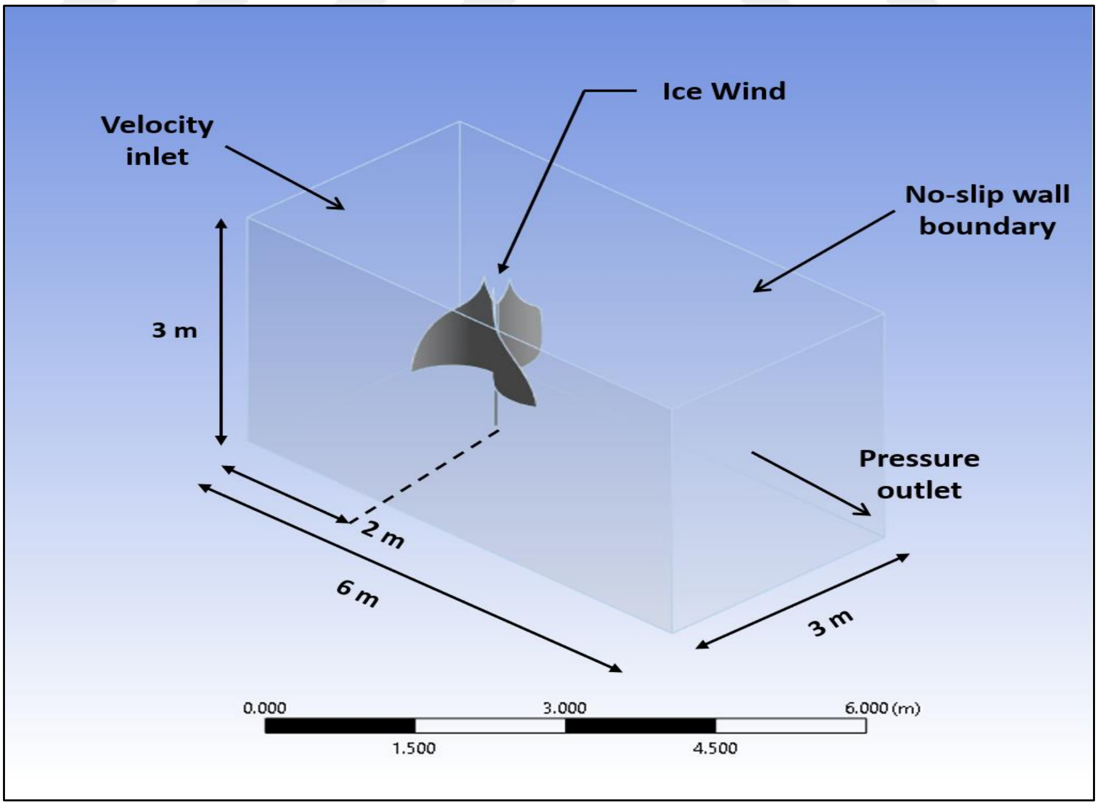

Figure 3.8 Computational Domain of the IceWind Turbine Model in ANSYS

A static mesh was used to perform a steady-state aerodynamic analysis. Tetrahedral mesh was applied due to handling complex geometries. The mesh consisted of 861,882 nodes and 4,790,485 elements. These numbers are required for precise flow analysis.

The turbulence model applied in this study is the shear stress transport SST k-ω. This model provides accurate predictions across different tip speed ratios. RANS method is selected because it takes less computational cost with validated results. All equations for numerical simulation and theoretical calculations will be shown later in Section 3.7.

As shown in (Figure 3.9), the mesh of the IceWind turbine from a side view. The solution methods used to solve the RANS equations are presented in table 3.4.

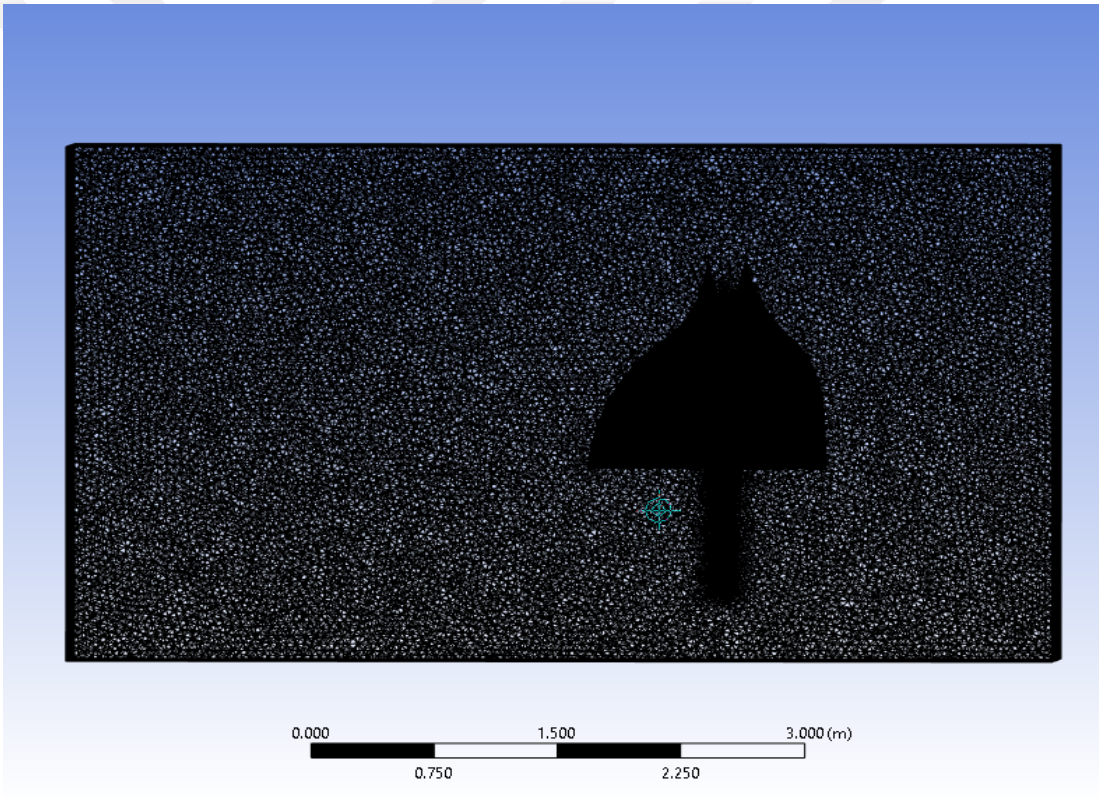

Figure 3.9 IceWind Turbine Model Mesh in ANSYS

Table 3.4 Numerical Solution Approach

Soultion aspect	Selected approach
Pressure-velocity coupling	Coupled scheme
Gradient	Least squres cell-based
Turbulent kinetic energy (k)	Second-order upwind scheme
Specific dissipation rate (ω)	Second-order upwind scheme
Pressure	Second-order upwind scheme
Momentum	Second-order upwind scheme

- **Setting Ice-Wind Turbines on the Building**

On the roof of the building, a concrete circle is designed, centered in the middle and supported by concrete columns. The large concrete circle can accommodate twenty vertical axis wind turbines. A second concrete circle is positioned at the center, on which fifteen vertical wind turbines can be installed. On the sides of each corner of the building there is a quarter circle, on each of which three turbines can be installed. The roof of the building was equipped with 42 vertical axis wind turbines. The concrete circles are designed to take into account the distance between one turbine and another. The distance between two consecutive turbines should not be less than one and a half times the diameter of the turbine to avoid aerodynamic interference between them [61].

(Figure 3.10) presents the distribution of turbines on the roof of the residential building. The turbines are distributed at three different heights. This arrangement improves the ability to capture wind from various directions.

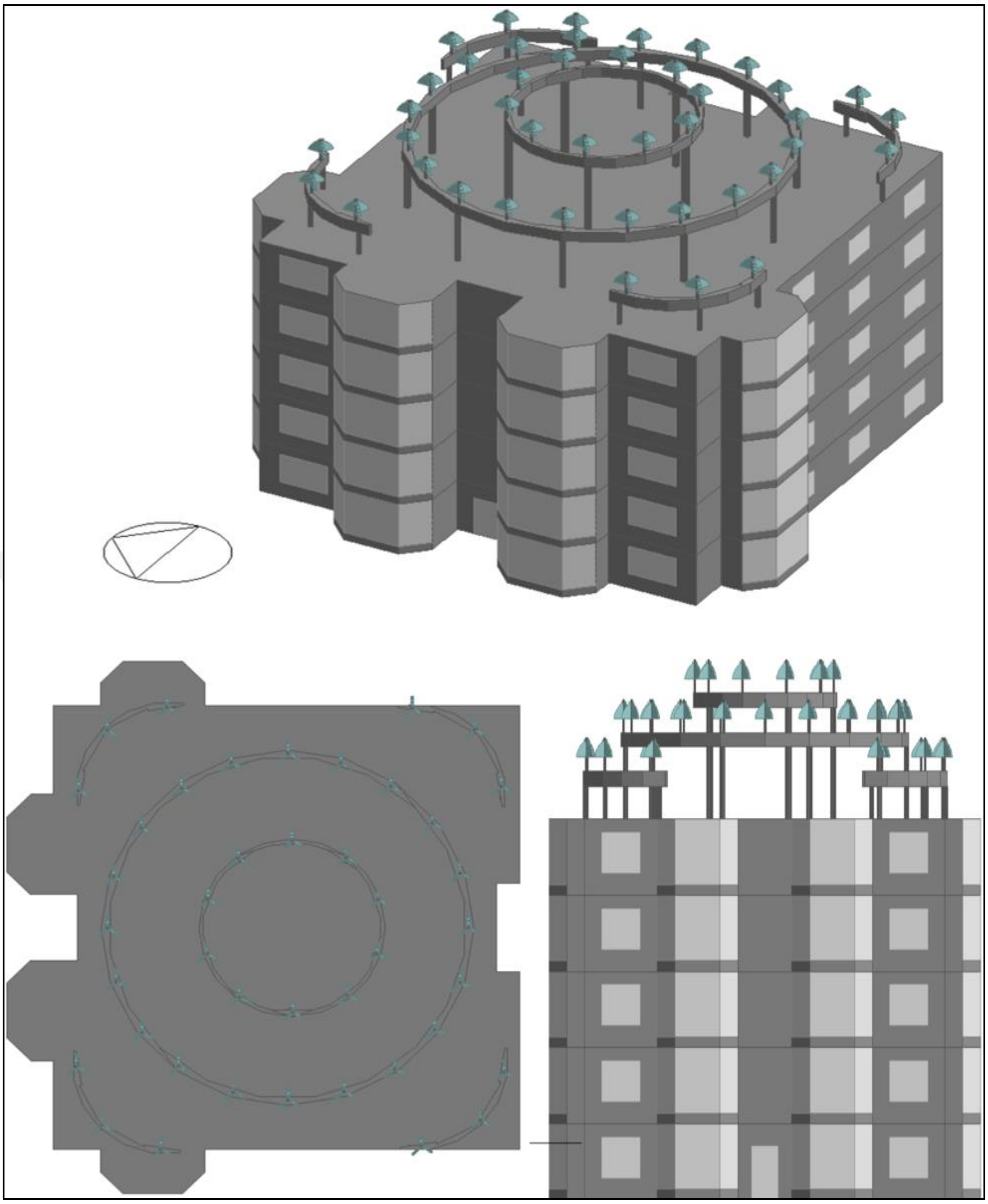

Figure 3.10 Ice-Wind Turbines Mounted on the Building (Developed by Author)

3.4.2 Case Two (Case 2): Building-Integrated Helical Wind Turbine

- **Helical Wind Turbine Design**

A helical vertical axis wind turbine is considered a lift-type turbine. This lift force allows the turbine to achieve higher efficiency. The helical shape reduces torque variations. Every airfoil has a unique shape and thickness. Some common types include NACA, EPPLER, and CLARK. The National Advisory for Aeronautics

(NACA) airfoils are the most widely used. NACA conducted experiments on various airfoil shapes, most of which are in use today. The NACA 0021 airfoil type was used in the turbine design. According to several previous studies comparing the efficiency of helical-type vertical axis wind turbines, the optimal results were obtained using NACA 0021 type airfoil [62-66]

This turbine is designed with three blades. The blades are bent at a 60° angle which enhances wind capture more efficiently than straight-blade. SolidWorks software was used in the design of the turbine as shown in (Figure 3.11). The rotor diameter and blade length are, respectively, D = 1.515 m and H = 1.52 m. The additional features of the helical turbine can be found in table 3.5.

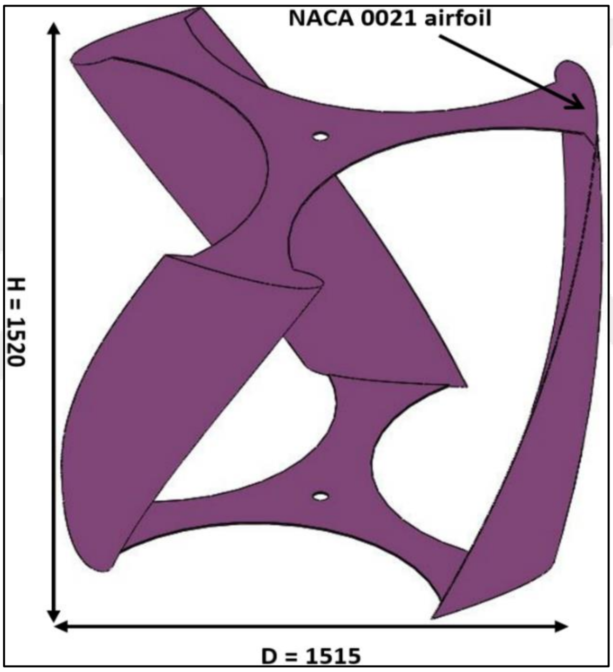

Figure 3.11 Helical Wind Turbine Dimensions (All Units Are in mm)

Table 3.5 Helical Rotor Parameters

Parameter	Value/Specefication	units
Airfoil profile	NACA 0021	-
Blade number (N)	3	-
Rotor diameter (D)	1.515	m
Rotor height (H)	1.520	m
Chord length	0.150	m
Solidity	0.594	-

- **Setting Computational Domain and Mesh Generation**

In this case, Finite Volume Fluent solver has been conducted, using shear stress transport SST k-ω. A 3D numerical simulation was performed. The domain has the following dimensions: 4 m height, 5 m width, and 9 m length. The turbine is positioned 3 m from the inlet velocity boundary and 6 m from the outlet pressure boundary. All other domain boundaries are treated as no-slip walls. (Figure 3.12) provides the defined computational domain used for the helical turbine .

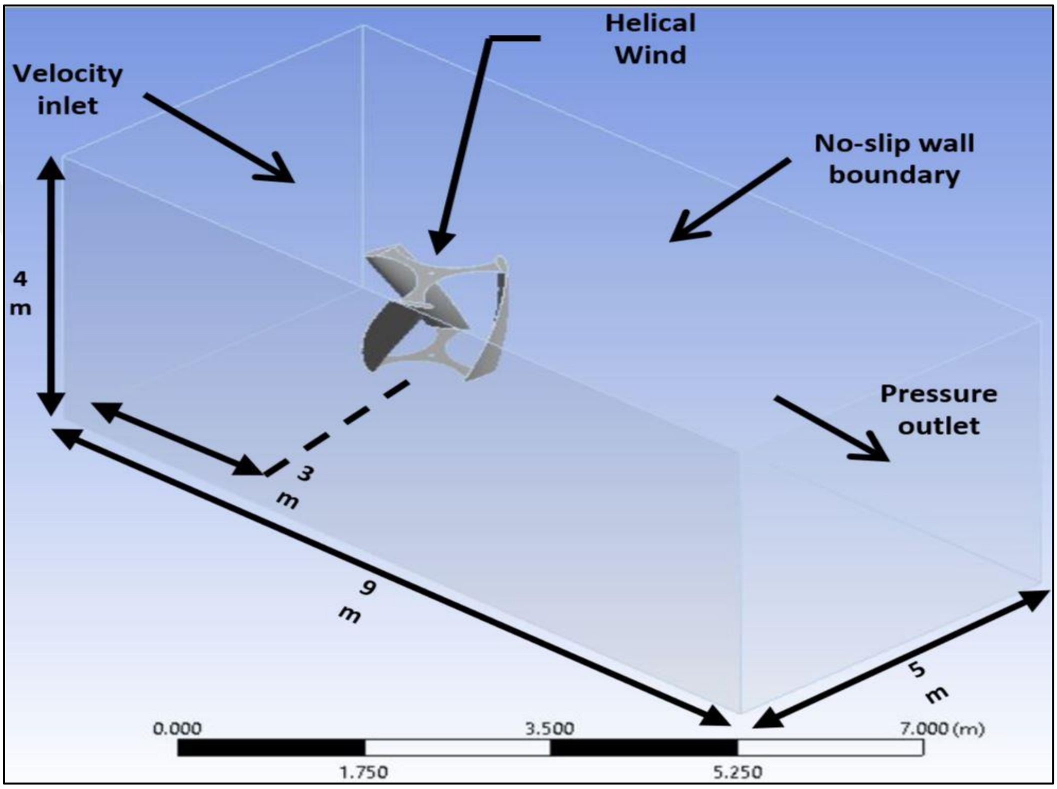

Figure 3.12 Computational Domain of the Helical Turbine Model in ANSYS

Steady-state simulation was used to analyze the long-term efficiency of the turbine at the lowest possible cost. The pressure outlet was set to zero-gauge pressure. The velocity inlet was assigned a uniform wind speed of 13 m/s. The nodes and elements were calculated as 777,032 and 4,232,347, respectively. (Figure 3.12) presents the mesh of the helical turbine.

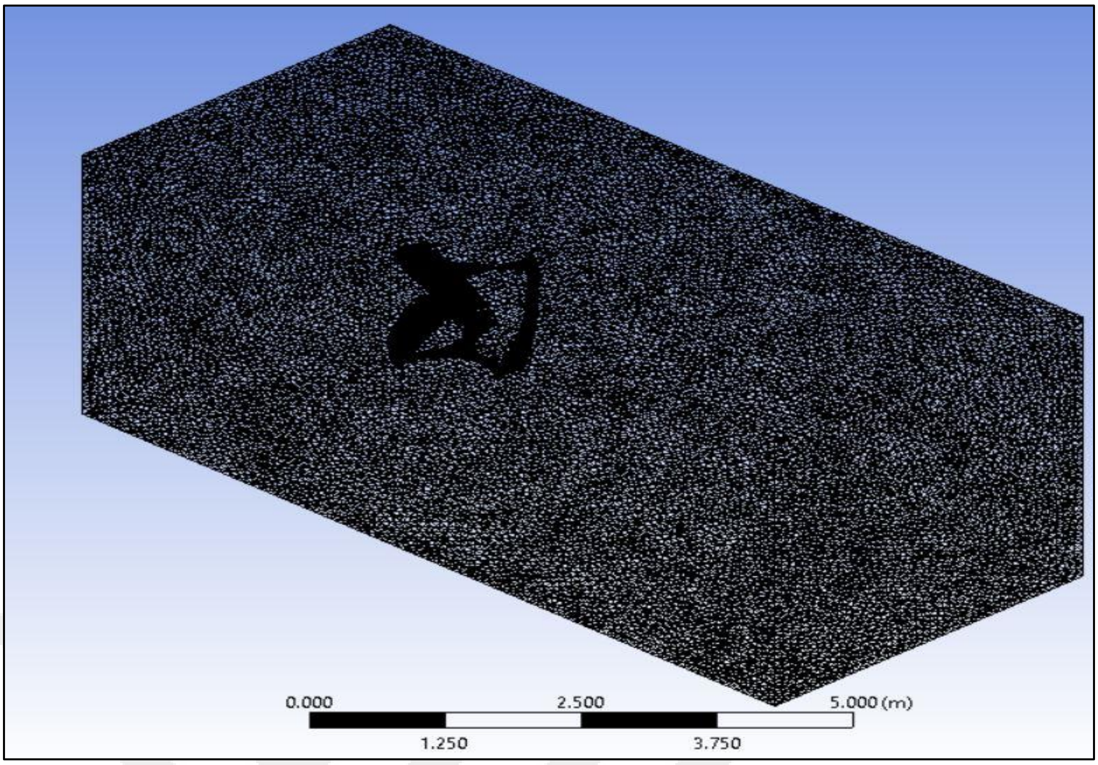

Figure 3.13 Helical Turbine Model Mesh in ANSYS

- **Setting Helical Wind Turbines on the Building**

The helical vertical axis wind turbines were installed on the concrete circles in the same manner as previously described. Forty-two helical turbines were closely spaced at three different heights. (Figure 3.14) shows the final installation of the helical turbines on the roof of the residential building.

Fixed-speed variable pitch is considered as power control for wind turbine. In this type of control, the turbine operates at a fixed speed while maintaining a variable angle of attack. The angle of attack was reduced to protect the turbine from the impact of high wind speeds.

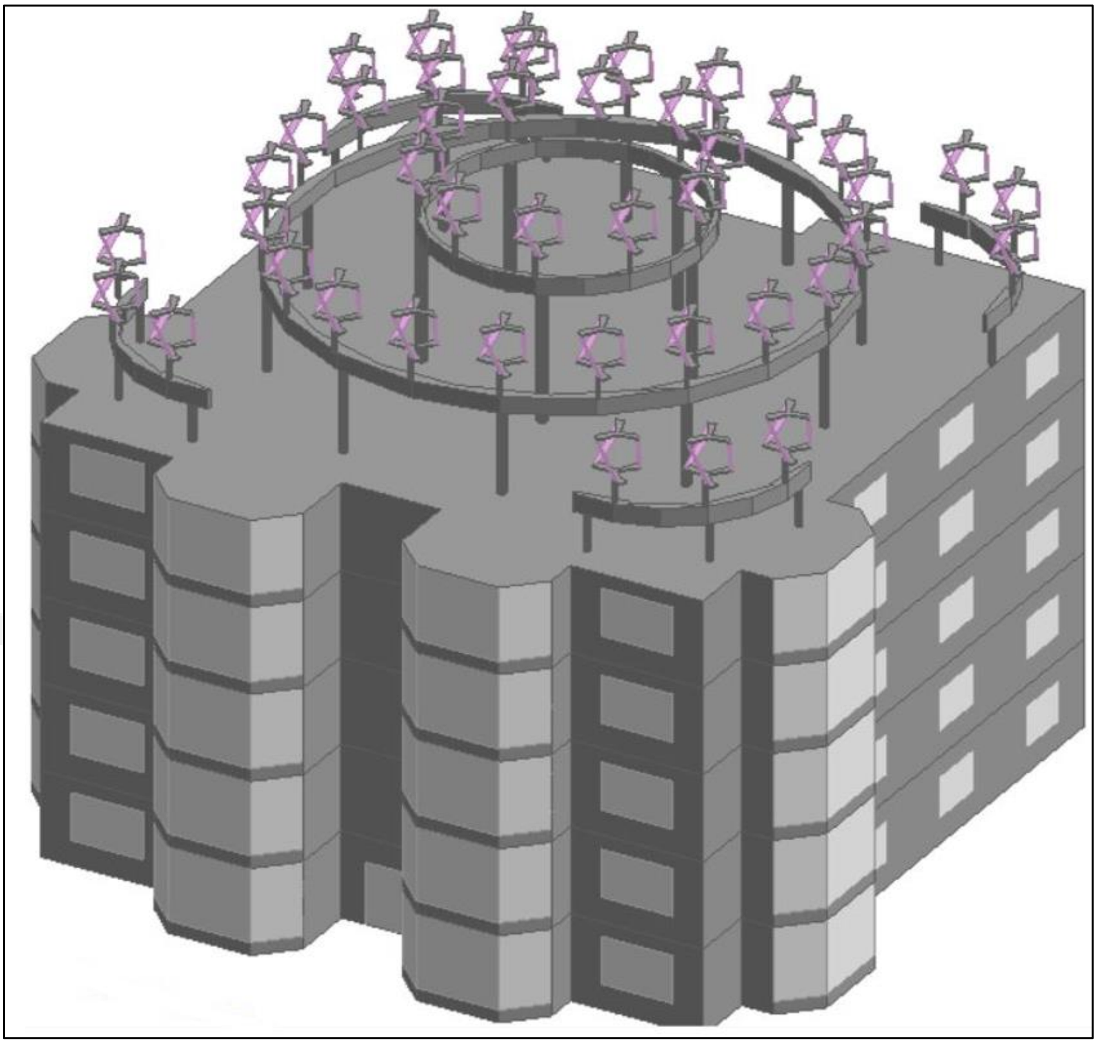

Figure 3.14 Helical Turbines Mounted on the Building (Developed by Author)

3.4.3 Case Three (Case 3): Building-Integrated Combined Wind Turbine

- **Combined Wind Turbine Design**

In this case, a combined design was studied, including two types: the helical-type, which is a three-blade lift-based, and the IceWind-type, which is a three-blade drag-based. A 50% measurement of the IceWind turbine mentioned earlier in the second case was taken. It was positioned centrally around the axis of rotation, with three helical blades bent at a 60° angle. (Figure 3.15) illustrates the design of the combined wind turbine.

This design combined two different types of vertical axis wind turbines, which improved the efficiency of capturing winds from all directions. The drag-based turbine can start at low speeds, while the lift-based turbine requires high speeds.

Combining these two types provides the advantage of self-starting capability and high efficiency. The turbine was designed using SolidWorks software. Table 3.6 summarizes the detailed dimensions of the turbine.

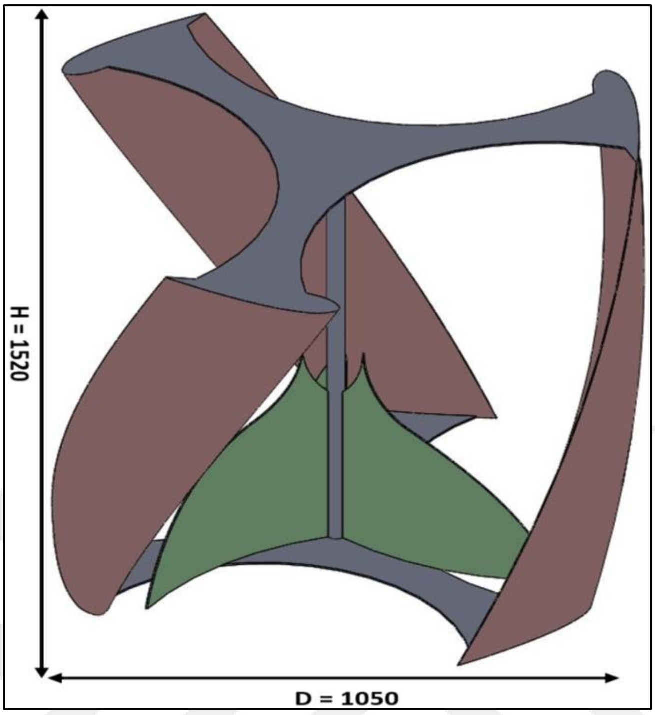

Figure 3.15 Combined Wind Turbine Dimensions (All Units Are in mm)

Table 3.6 Geometric Design and Performance Parameters of the Combined Wind Turbine

Parameter	Value/Specefication	units
Airfoil profile	NACA 0021	-
Blade of inner IceWind	Semicircle	-
Diameter of inner IceWind	0.7575	m
Diameter of outer Helical turbine	1.05	m
Height of IceWind	0.75	m
Height of Darrieus (Helical)	1.52	m
Total swept area	1.45	m^2
Freestram velocity	7	m/s

- **Setting Computational Domain and Mesh Generation**

The computational domain for this simulation measures 9 m in length, 5 m in width, and 4 m in height. Two mesh sizes were used for computational domain. The domain body mesh was set to 0.07 m, while the turbine body mesh was 0.01 m. This setup improves accuracy. A finer mesh is focused on the combined turbine, which is the main area of interest. The mesh consists of 965,768 nodes and 5,419,664 elements. (Figures 3.16 and 3.17) present the domain defined and mesh setup, in sequence.

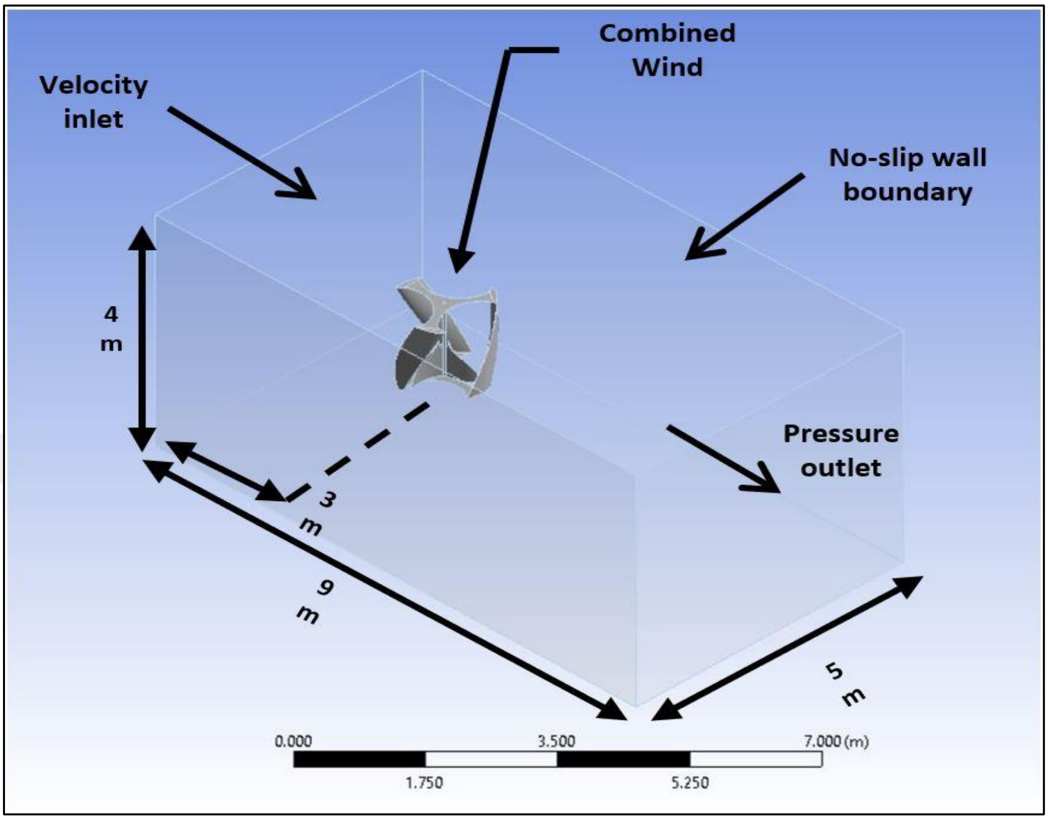

Figure 3.16 Computational Domain of the Combined Turbine Model in ANSYS

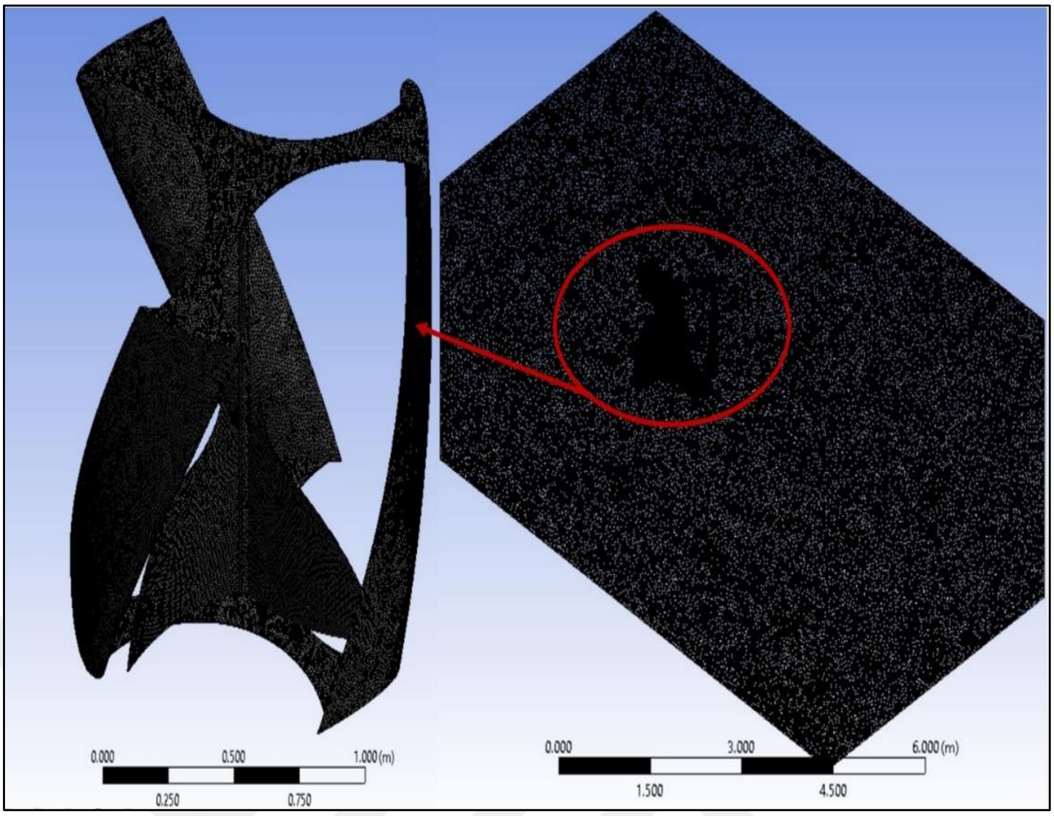

Figure 3.17 Combined Turbine Model Mesh in ANSYS

- **Setting Combined Wind Turbines on the Building**

The turbines were mounted on the roof of the residential building in the same manner as previously mentioned in sections (3.4.1) and (3.4.2). Forty-two combined vertical axis wind turbines were distributed with optimized spacing to prevent aerodynamic interference. (Figure 3.18) illustrates the locations of the turbines on the building's roof.

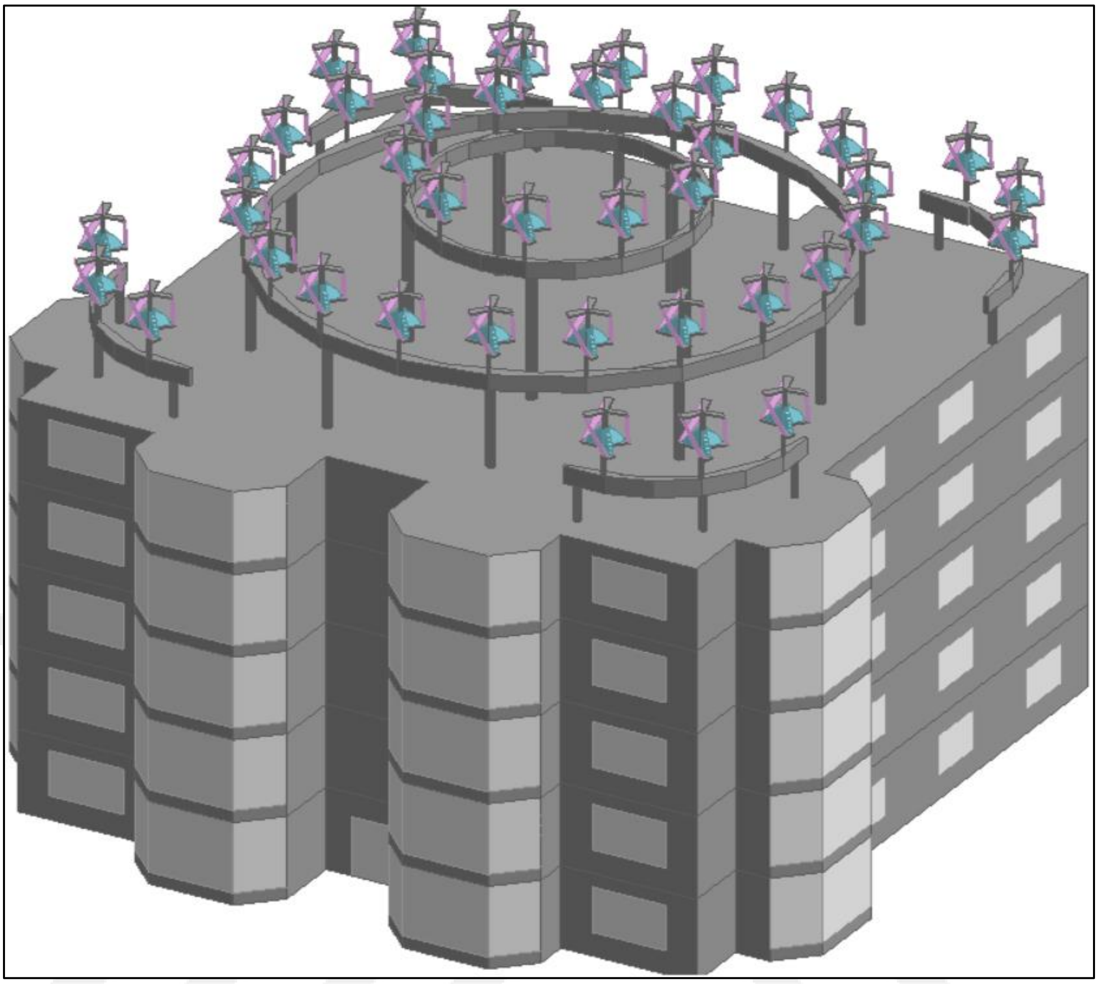

Figure 3.18 Combined Turbines Mounted on the Building (Developed by Author)

3.5 Input Parameters of Wind Turbine

After designing the three vertical axis wind turbines in SolidWorks software, the appropriate domain dimensions were determined based on the turbines' designs. Numerical simulation was performed in ANSYS Fluent software. Table 3.7 shows the analytical results for the mesh quality of each turbine.

Table 3.7 Summary of Mesh Quality

Wind Tubrine Type	Number of Nodes (N)	Number of Elements (E)
IceWind VAWT	861,882	4,790,485
Helical VAWT	777,032	4,232,347
Combined VAWT	965,768	5,419,664

It is worth noting that the basic information required to simulate turbines within the DesignBuilder software are two wind values. One is to enter the local average wind value, which in our study was estimated at approximately 7 m/s. The second value is the rated wind speed, which was adopted in this study for most small-scale wind turbines, 13 m/s, according to the IEC 61400-2 regulation.

Each turbine type was simulated within the DesignBuilder software to determine how efficiently it reduced energy consumption within the residential building. Table 3.8 presents all the input parameters for the three types of wind turbines within the DesignBuilder software.

Table 3.8 Input Parameters

Input Parameter	Value/Specefication	Units
Operation type	24/7	-
Power control	Fixed speed variable pitch	-
Rotor speed	159/177/191	rev/min
Rotor diameter	1.515/1.515/1.05	m
Number of blades	3/3/6	-
Rated power output	430/350/590	W
Rated wind speed	13	m/s
Cut out wind speed	3.5	m/s
Cut in wind speed	25	m/s
Maximum tip speed ratio	1.8/2/1.5	-
Maximum power coefficient	0.17/0.21/0.31	-
Annual local average wind speed	7	m/s

3.6 Cost Analysis

Economic viability is one of the most important factors to consider when designing a wind turbine [67-68]. Sometimes a turbine can be highly efficient, but the materials used in its manufacture are expensive, making it economically unviable. When designing any wind turbine, there are certain calculations that can be used to determine its life cycle. These calculations are referred to as the payback period analysis.

The stages of payback period analysis for the wind turbine are as follows:

1. Calculating the total energy of the wind turbine.
2. Calculate annual energy production from the total power output.
3. Estimate electricity cost savings.

4. Evaluate investment and maintenance cost.
5. Compute the payback period by dividing the initial investment by the net annual savings.

The economic analysis of the turbines revealed distinct differences in their initial costs, maintenance expenses, and overall payback periods. Across all cases, the local electricity price of $0.07 per kWh and an annual maintenance cost of $75 per turbine were considered in the calculations.

The initial investment costs for the IceWind VAWT, helical VAWT, and combined VAWT are 2000, 1800, and 3000 USD, respectively. All equations of the payback period are explained in the next section.

3.7 Equations

In this section, all the numerical and theoretical calculations of the shear stress transport SST k-ω equations, wind turbine performance, and payback period of the turbines are discussed.

$$\frac{\partial}{\partial t}(\rho k) + \frac{\partial}{\partial x_i}(\rho k u_i) = \frac{\partial}{\partial x_j}\left(\Gamma_k \frac{\partial k}{\partial x_j}\right) + G_k + Y_k + +S_k + G_b \tag{3.1}$$

$$\frac{\partial}{\partial t}(\rho \omega) + \frac{\partial}{\partial x_i}(\rho \omega u_i) = \frac{\partial}{\partial x_j}\left(\Gamma_\omega \frac{\partial \omega}{\partial x_j}\right) + G_\omega + Y_\omega + +S_\omega + G_{\omega b} \tag{3.2}$$

In these equations, Y_k and Y_ω represent the dissipation of k and ω due to turbulence. S_ω and S_k are user-defined source items. $G_{\omega b}$ and G_b account for buoyancy terms. Γ_ω and Γ_k represent the effective diffusivity of ω and k, respectively. G_ω represents the generation of ω. G_k represent the generation of turbulence kinetic energy due to mean velocity gradients [69].

- **Wind turbine performance and power equations**

The power coefficient, tip speed ration, and solidity are determined using the following equations, respectively.

$$C_P = \frac{P_{Turbine}}{P_{available}} = \frac{P_{Turbine}}{0.5\rho A_S V^3} \tag{3.3}$$

$$\lambda = \frac{\omega R}{V} \tag{3.4}$$

$$\sigma = \frac{N.c}{R} \tag{3.5}$$

$P_{Turbine}$: Power output (W)

ρ: Air density (kg/m^3)

A_S: Swept area (m^2)

V: Wind speed (m/s)

R: Radius of the rotor (m)

ω: Angular velocity (rad/s)

N: Number of the blades

c: Chord length of the blade (m)

- **Payback period analysis**

The following equations are used to calculate the payback period. These equations provide a step-by-step framework or evaluating the financial performance of the vertical axis wind turbines.

$$P_{total} = P_{turbine} \times N_t \tag{3.6}$$

$$E_{annual} = \frac{P_{total} \times H}{1000} \tag{3.7}$$

$$S_{annual} = E_{annual} \times C_{electricity} \tag{3.8}$$

$$I_{total} = C_{turbine} \times N_t \tag{3.9}$$

$$C_{maintenance} = C_{maintenance\ per\ turbine} \times N_t \tag{3.10}$$

$$S_{net} = S_{annual} - C_{maintenance} \tag{3.11}$$

$$T_{Payback} = \frac{I_{total}}{S_{net}} \tag{3.12}$$

Where:

$P_{turbine}$: Power output of a single turbine (W)

P_{total}: Total power output (W)

N_t: Number of turbines

E_{annual}: Annual energy production (kWh/year)

$C_{electricity}$: Electricity price (USD/kWh)

$C_{turbine}$: Cost of a single turbine (USD)

$C_{maintenance}$: Maintenance cost per turbine (USD/year)

S_{annual}: Annual savings in electricity cost (USD/year)

$T_{Payback}$: Payback period (years)

I_{total}: Total initial investment (USD)

S_{net}: Net annual savings (USD/year)

CHAPTER 4

RESULTS AND DISCUSSIONS

This chapter consists of two sections. The first section discusses the numerical results obtained from ANSYS Fluent software. All results were obtained under the wind speed of 13 m/s. The simulation results include contour plots of dynamic pressure, static pressure, and velocity magnitude around the turbine blades. Additionally, the analysis of the residential building obtained from the DesignBuilder software is presented, showing the distribution of temperatures, pressures, and velocities inside the residential building. The second part of this chapter includes the energy reduction value for each type of wind turbine used and its efficiency. A comprehensive comparison of each wind turbine type is also provided.

4.1 CFD Analysis and Building Performance

4.1.1 CFD Analysis of The Wind Turbines

Three numerical analyses are adopted to examine the flow patterns and their impact on wind turbines using contour results.

- **Dynamic Pressure Contours**

Figures (4.1), (4.2) and (4.3) represent the dynamic pressure contours in both rotor domain and the wind blades for IceWind, helical, and combined VAWTs. A low-pressure area develops on the side of the proceeding blade, enhancing the torque produced by the rotating rotor.

The first case in (Figure 4.1) shows the dynamic pressure distribution around the IceWind-type wind blades. It is noted that the highest dynamic pressure was found on the convex side towards the wind, while the lowest pressures can be observed on the convex side of the turbine blades. In other words, the side of the turbine that faces the incoming air is exposed to higher pressure, whereas the opposite side experiences lower pressure values.

(Figure 4.2) represents the dynamic pressure distribution around the helical wind blades. The highest dynamic pressures are observed near the blade tips. This can be attributed to the efficient capture of wind energy as the airflow decelerates when interacting with helical blades. In contrast, low pressure wake zones downstream indicate that energy has been captured.

(Figure 4.3) illustrates the dynamic pressure distribution of the combined vertical axis wind turbine, which boasts a higher wind capture efficiency than the previous two models, the IceWind and Helical VAWTs. High dynamic pressures can be observed near the blade interaction zones, enhancing rotation and improving wind energy capture. The extended low-pressure wake indicates more efficient energy extraction compared to using only one turbine type.

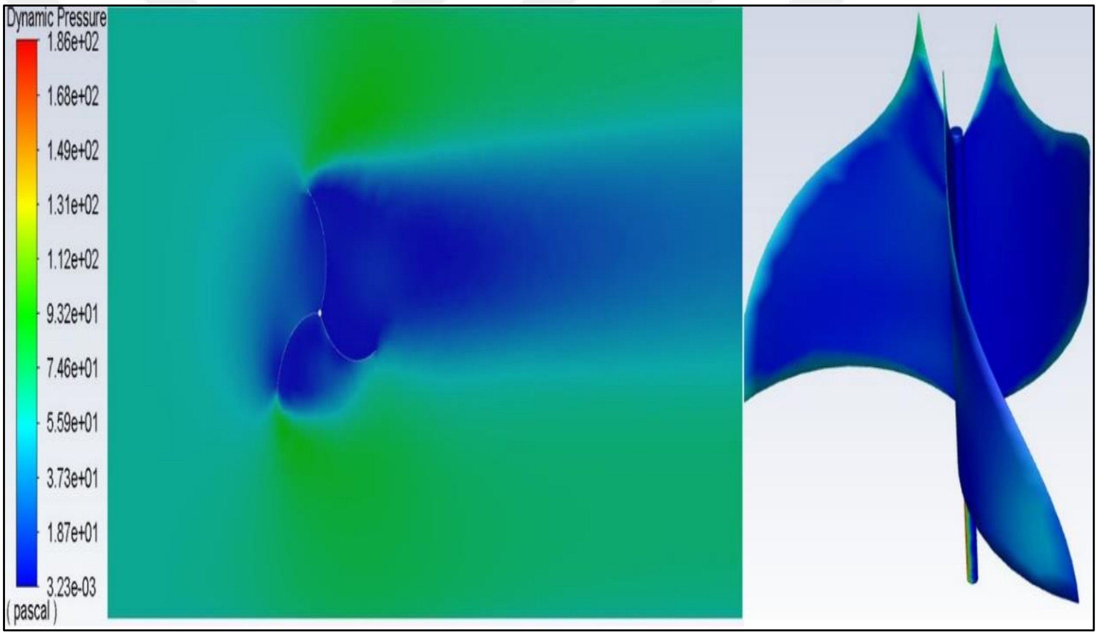

Figure 4.1 Dynamic Pressure Contour Plot of the IceWind Turbine

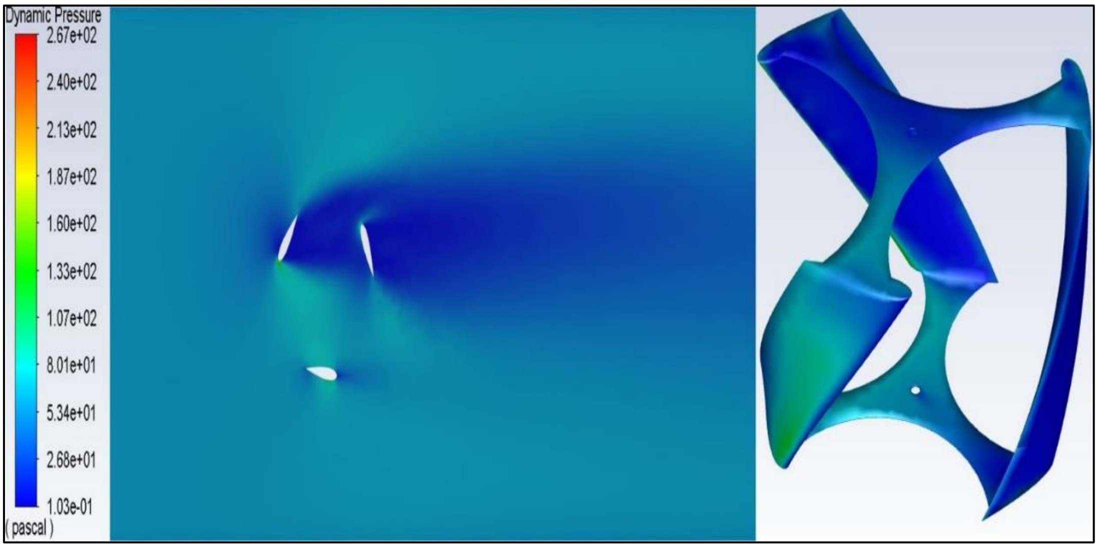

Figure 4.2 Dynamic Pressure Contour Plot of the Helical Turbine

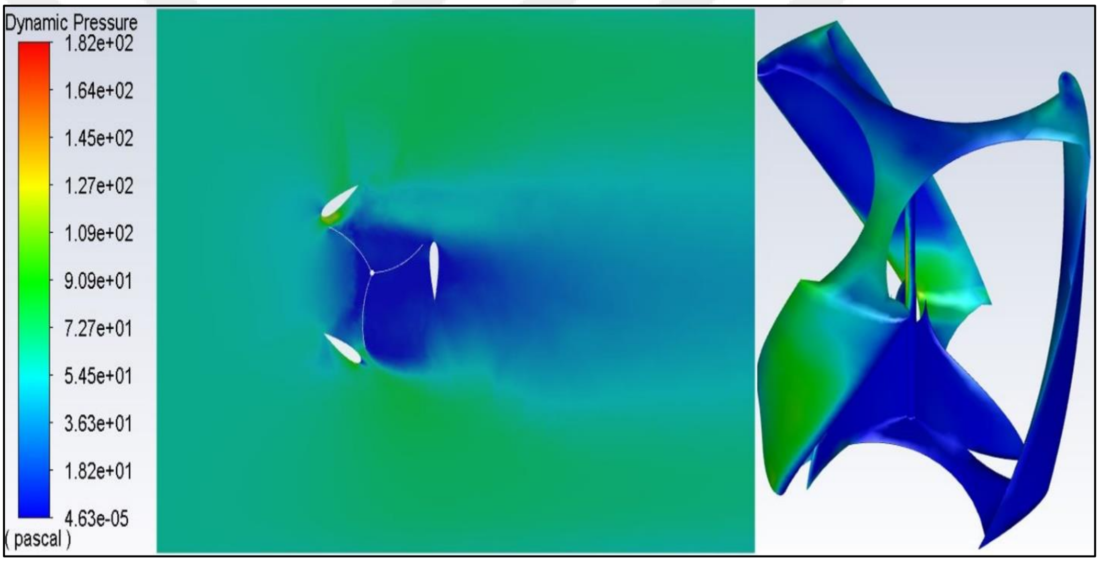

Figure 4.3 Dynamic Pressure Contour Plot of the Combined Turbine

- **Static Pressure Contours**

Figures (4.4), (4.5), and (4.6) show static pressure analyses for the three wind turbines. In all cases, high static pressure regions occur near the leading edges of the turbine blades as a result of airflow velocity decrease upon impact with the turbine blades. Conversely, low pressure zones in the wake, result from flow acceleration and separation.

(Figure 4.4) shows that the IceWind-type turbine reached a maximum static pressure of nearly 76.8 Pa. This suggests that the turbine performs effectively under the current flow conditions. On the other hand, as seen in (Figure 4.5), the helical VAWT reached a maximum of around 67.4 Pa. The regular gradient in pressure helps maintain steady performance.

For the combined type in (Figure 4.6) maximum static pressure can be observed near the leading edges of both types. The asymmetric pressure distribution emphasizes the interaction between the wind blades, enhancing torque generation and lift. The highest value of the static pressure achieved for the combined VAWT was approximately 80 Pa.

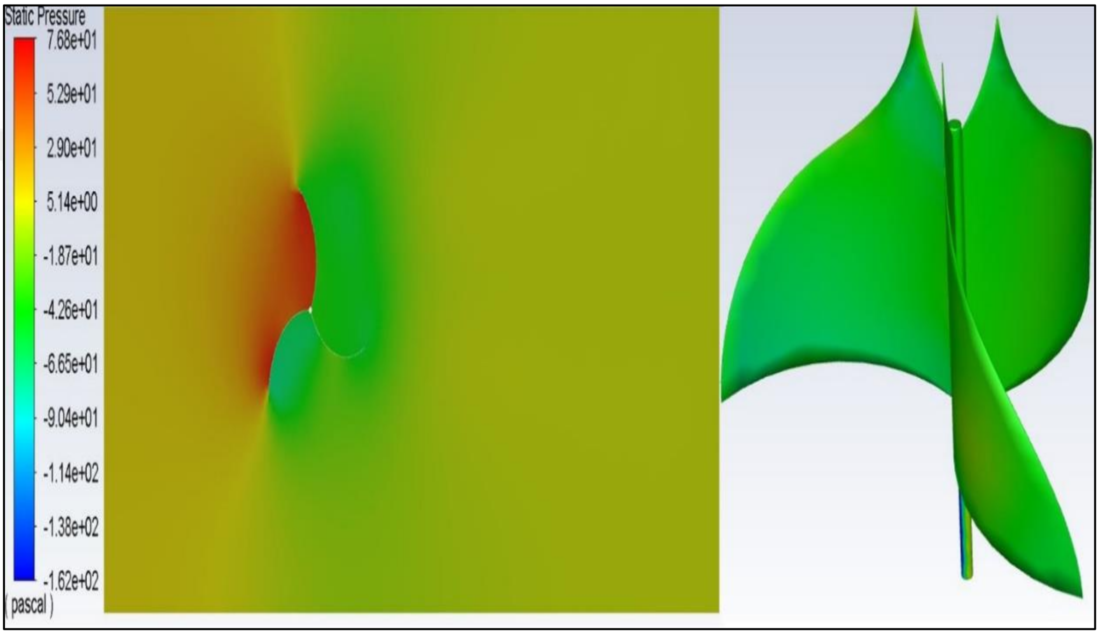

Figure 4.4 Static Pressure Contour Plot of the IceWind Turbine

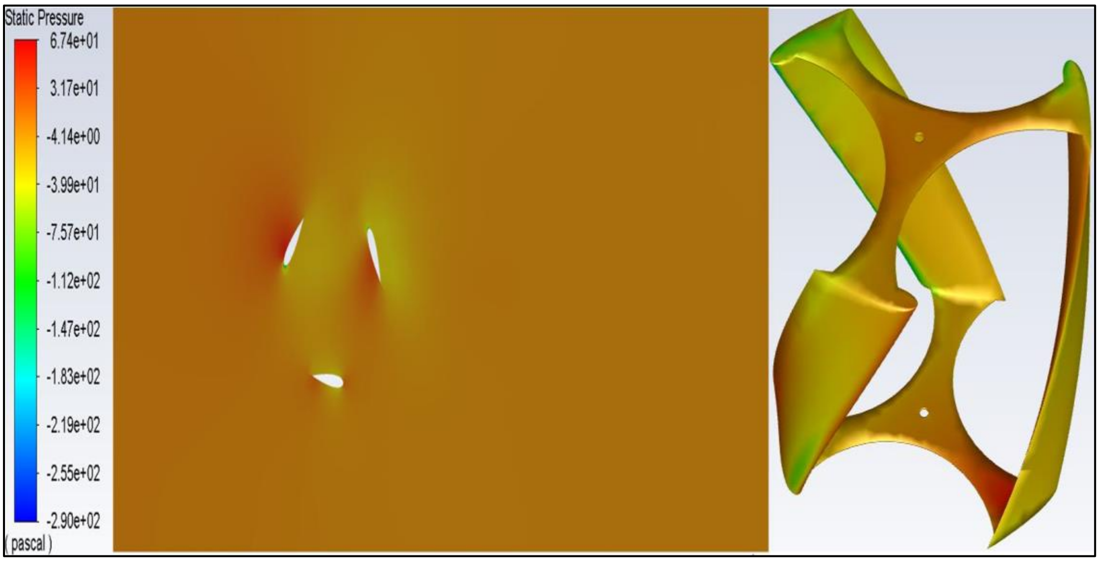

Figure 4.5 Static Pressure Contour Plot of the Helical Turbine

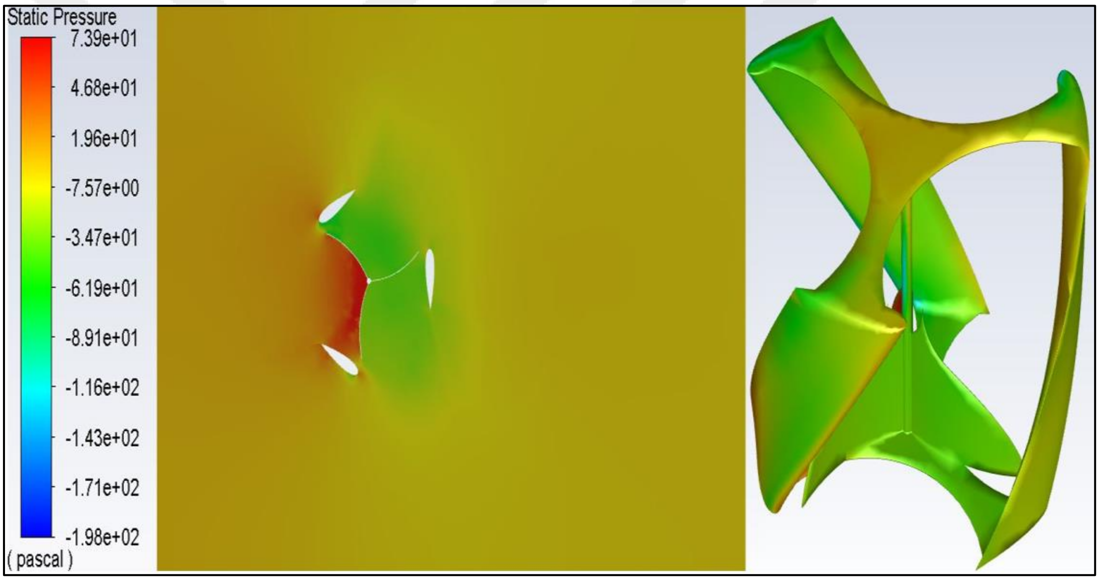

Figure 4.6 Static Pressure Contour Plot of the Combined Turbine

- **Velocity Contours**

Figures (4.7), (4.8), and (4.9) represent the velocity contours around the wind turbines blades. In the IceWind turbine, it can be observed that the highest velocities were recorded at the tip blades. On other hand, Low velocities can be seen in the wake zone, and this is due to increased turbulence. The maximum velocity observed for the IceWind turbine was 16.5 m/s as shown in (Figure 4.7).

It can be observed that the higher relative velocities are recorded compared to the helical turbine, due to the fact that the helical type, known as a lift-based wind turbine, as shown in (Figure 4.8), produced greater flow velocities in comparison to the IceWind-type, which is a drag-based wind turbine. In addition, the IceWind's structure maintains more stable wake. While the helical type has less interaction with the wind flow, as the wind-catching areas are less obstructive than in the IceWind -type, and the addition of this design induces more turbulent wake regions.

(Figure 4.9) represents the velocity distribution for the combined VAWT. The maximum velocities are observed in the wind capture zones of the helical and IceWind blades. The maximum velocity recorded was approximately 17 m/s. Stronger vortices are revealed in the combined turbine more than in the two previous types. This indicates better energy capture, which improves overall turbine performance.

In conclusion, using the static mesh type and setting the domain dimensions relative to the turbine dimensions as described in the previous studies for [26, 31]. The results were obtained for the pressure and velocity distributions of the three wind turbines. The power coefficient values for the IceWind, helical and combined turbines were determined as follows: 0.17, 0.21 and 0.31. The rated power of the Icewind turbine was calculated as 430 W. For the helical and combined turbines, the rated power values were found to be 350 W and 590 W, respectively.

Comparing previous studies mentioned in Chapter 2 yielded more efficient and accurate results. The current results present the analysis from both perspectives. Firstly, numerical verification was performed using the ANSYS Fluent software; secondly, turbine simulation was conducted to assess their energy efficiency annually using the DesignBuilder software. The results indicate that combining two types of turbines, one a lift-based and the other a drag-type, provides better results.

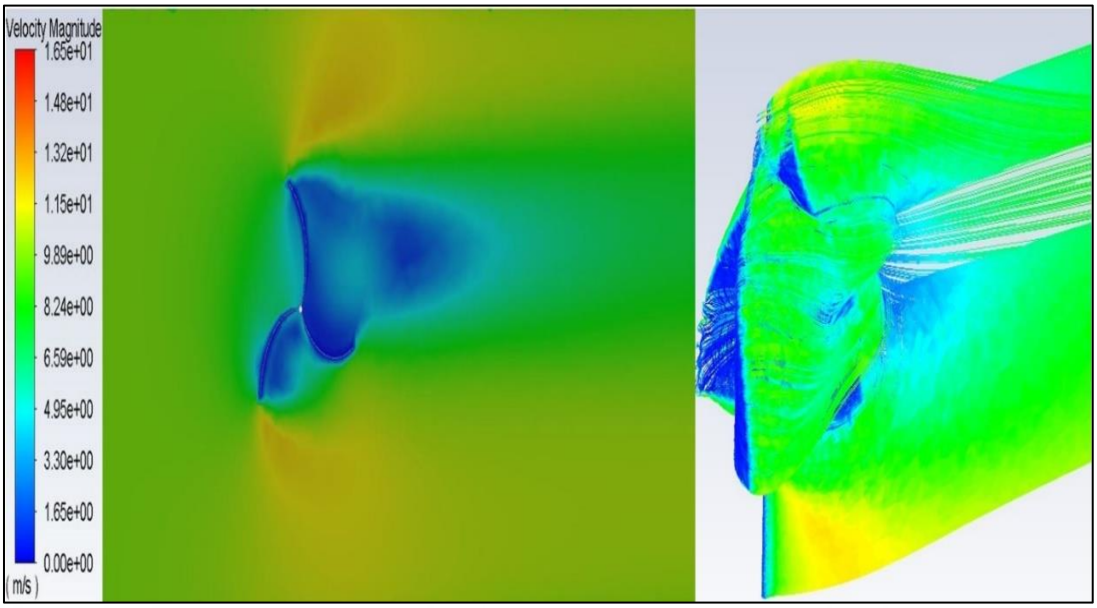

Figure 4.7 Velocity Contour Plot of the IceWind Turbine

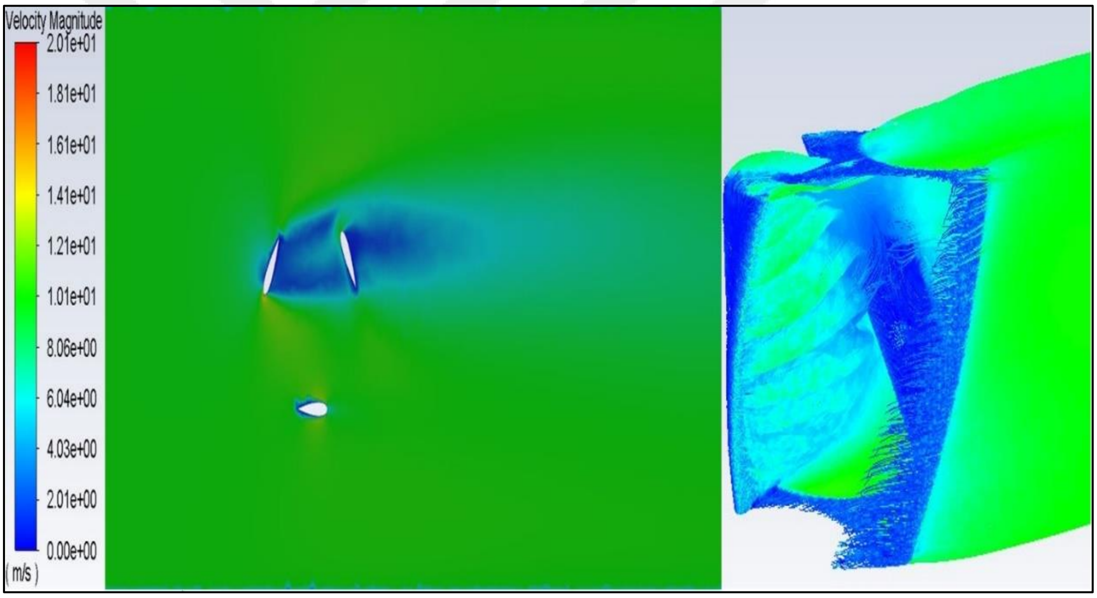

Figure 4.8 Velocity Contour Plot of the Helical Turbine

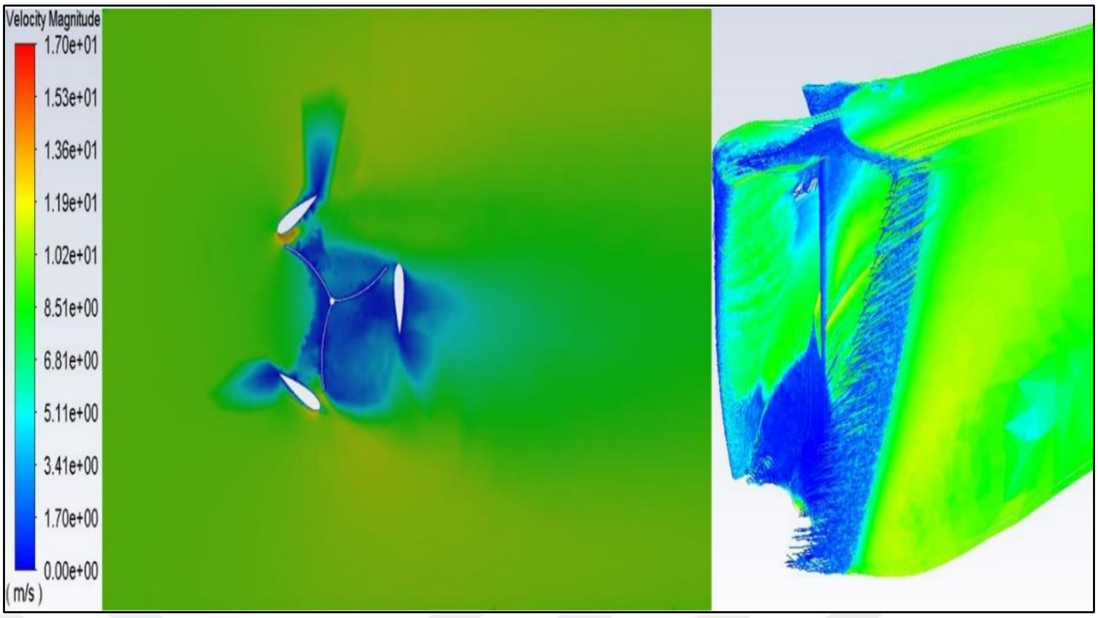

Figure 4.9 Velocity Contour Plot of the Combined Turbine

4.1.2 Indoor Climate and Comfort Analysis

Assigning significance to the external climate and internal thermal environment is crucial for understanding thermal performance, as the internal environment depends primarily on the external conditions. This analysis was conducted to determine the heat distribution and thermal comfort of the building. The analysis provides a comprehensive understanding of the materials used in the building and the validity of the simulation.

The overall temperature annually provides an understanding of the thermal comfort inside the residential dwelling. The thermal comfort can be observed to be around 19 °C, as shown in (Figure 4.10). This analysis presents the ideal simulation for the specified conditions in Izmir, Türkiye. The average temperature for this residential building, located in the Mediterranean climate, falls within this temperature range [70].

Temperatures observed near windows ranged from 14 to 16 °C because the airflow is more concentrated and convective cooling is enhanced. The result of the analysis shows that most zones inside the building are within 19 °C.

(Figure 4.11) shows the distribution of airflow velocity along the exterior perimeter of the residential building on all four sides. The maximum air velocity was measured near the windward-facing walls around 0.58 m/s. The wind reaches the building. As a result, the speed of the air near the surface drops significantly.

High-velocity regions indicate natural ventilation. In addition, low-velocity areas, ranging from 0.05 to 0.11 m/s, are concentrated in the interior of the residential building. These readings indicate ideally ventilated areas for indoor living. This velocity simulation indicates the importance of a building design that provides efficient natural ventilation and improves indoor air circulation.

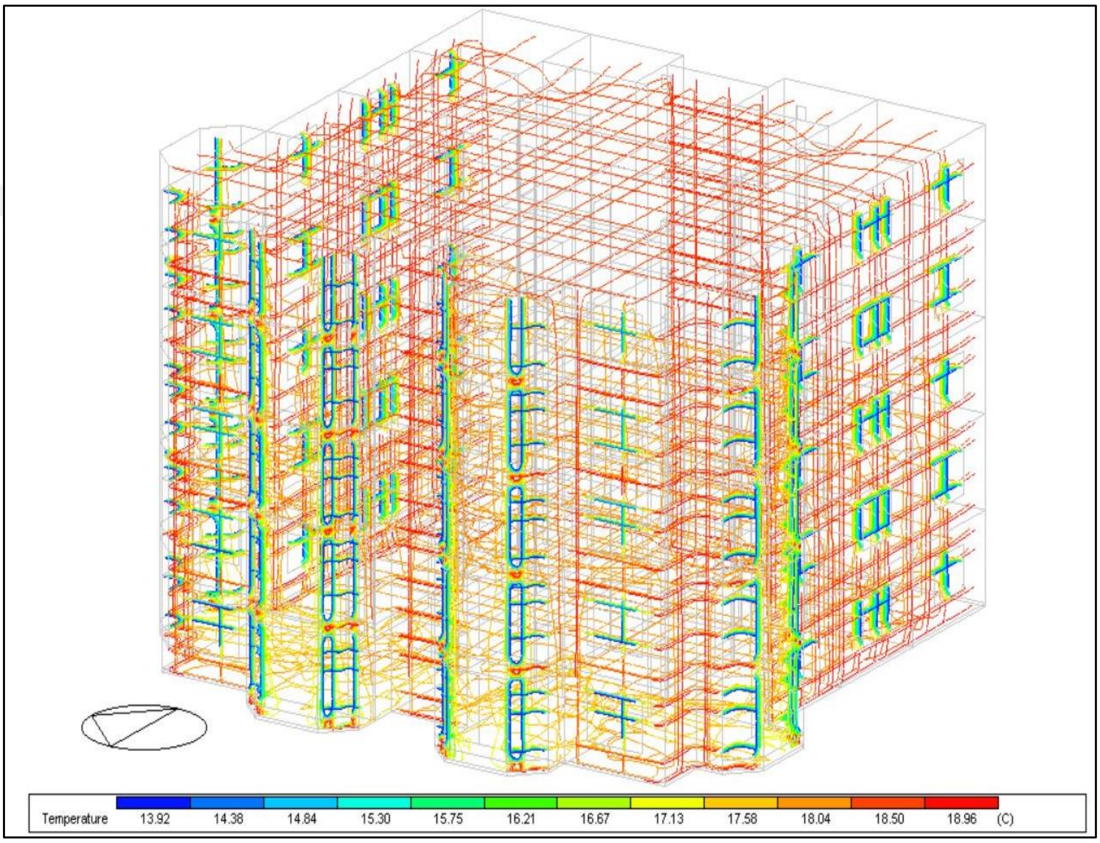

Figure 4.10 CFD Analysis of Indoor Thermal Distribution

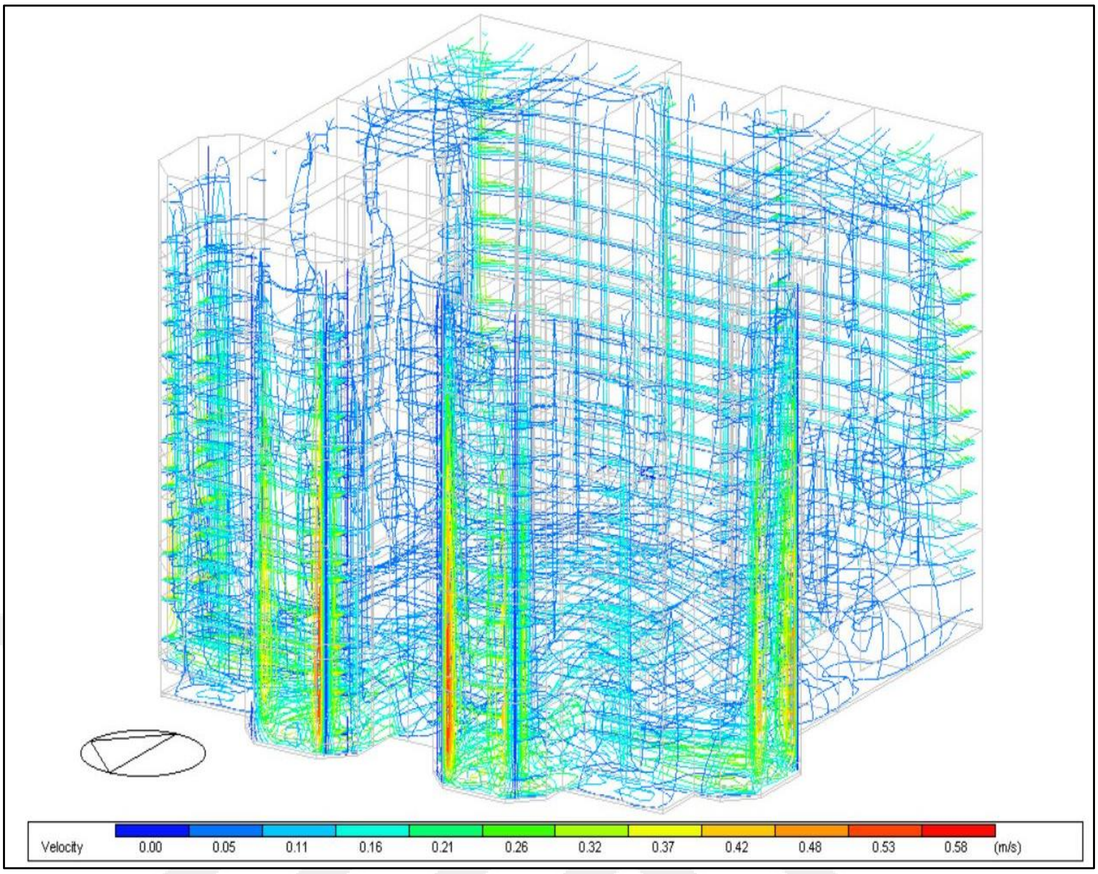

Figure 4.11 CFD Analysis of Indoor Airflow Velocity Distribution

4.2 Energy Savings and Payback Period Analysis

This section presents a detailed comparison of the three types of vertical wind turbines. The main comparison includes two sections: the first discusses the energy reduction results for each turbine type after simulating forty-two turbines on the rooftops of the residential building. The second section analyzes the payback period and economic feasibility results.

After running the simulation in DesignBuilder software, the total energy consumption of the residential building was found to be 172 kWh/m^2, without conducting any wind energy simulations. This result was obtained by simulating the weather annually, in addition to considering the building's area and materials used. The simulation also includes complex calculations related to the electrical appliances present in each zone of the building.

Simulation results for the IceWind turbines indicate a 22.93 % reduction in energy consumption, with a payback period of 10.60 years. On the other hand, the helical-type observed an 18.45 % decrease in energy consumption, with a payback period of 12.89 years. In contrast, the combined type contributed to a 30.88 % reduction in energy consumption, with a payback period of 10.49 years.

The results indicate that the best turbine in terms of energy consumption reduction and payback period is the combined VAWT. The IceWind turbine was the second most effective in reducing energy consumption, with a difference of approximately 8% compared to the combined type. Furthermore, the highest payback period was achieved by the Helical turbine. The payback period for the IceWind turbine was relatively similar to that of the Combined type.

(Figure 4.12) and table 4.1 summarize the final results of the study. A payback period calculation was performed using an electricity price of 0.07 kWh with a maintenance cost of approximately $75 for all turbine types. The initial cost of each IceWind turbine was $2,000. The IceWind turbine achieved moderate results in terms of energy consumption and payback period. The second model, the helical type, recorded lower efficiency compared to the IceWind and the combined turbines. The initial cost was estimated at $1,800 for each helical turbine. Despite the $200 lower cost than the IceWind type, it achieved a lower payback period compared to the other two types.

The optimal results were determined using the combined type, with an initial cost of $3,000. This cost is higher than the previous two types due to the turbine's complex shape and its inclusion of two different types of wind blades. The payback period was significantly lower than the helical type, at about 2.4 years, and slightly less than the IceWind-type.

In conclusion, the use of these three types of vertical axis wind turbines VAWTs in urban areas is essential for reducing energy consumption in residential buildings, especially in areas with moderate to high wind speeds, such as the Çeşme region of İzmir, Türkiye.

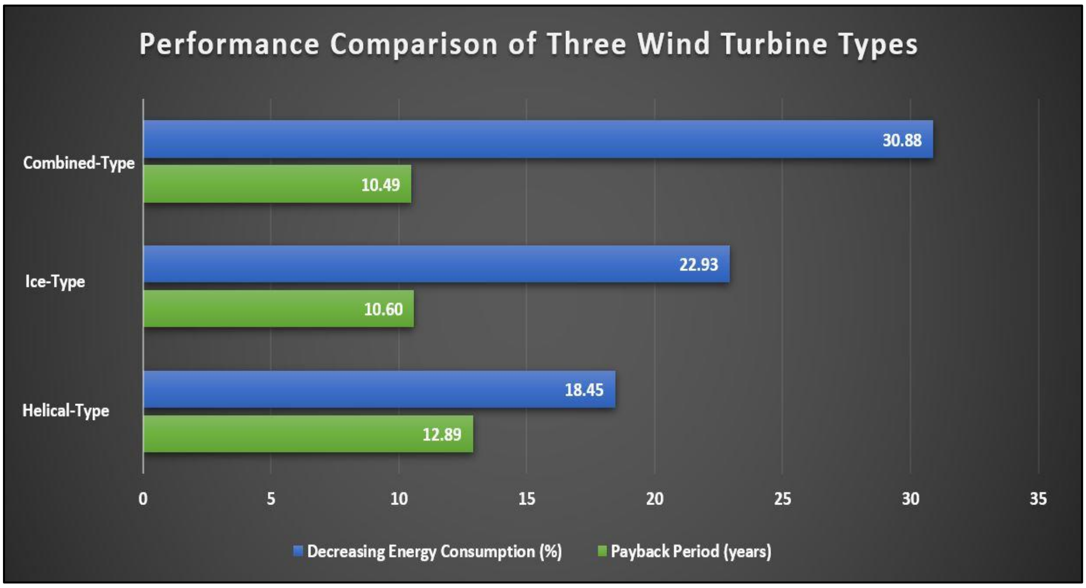

Figure 4.12 Comparison of Energy Savings and Payback Period for All Cases

Table 4.1 Simulation Results for All Cases

Model Name	Energy Consumption (kWh/m^2)	Energy Saving %	Payback Period (years)
Baseline model	172	-	-
Case 1	132.56	22.93	10.60
Case 2	140.27	18.45	12.89
Case 3	118.89	30.88	10.49

4.3 Limitations of the Study

Although many aspects were discussed and numerical simulations were performed for the three turbines, this study has certain limitations. The turbines were simulated only within the İzmir region; the study did not include a comprehensive simulation of other global regions such as parts of Europe or North America where some factors such as average wind speed and other weather conditions may vary. The turbines were simulated in the Ansys Fluent software using the number of nodes not exceeding 5.5 million elements due to computational limitations and the need to minimize simulation costs. More accurate results could be achieved, and the study brought closer to real-world conditions, through experimental methods. This could be done by fabricating a prototype with the dimensions specified in this study and testing it in a wind tunnel, instead of relying solely on numerical verification.

CHAPTER 5

CONCLUSION AND RECOMMENDATIONS

5.1 Summary of the Work

This study focused on the design and simulation of three vertical wind turbines on a residential building in the Çeşme, Izmir, Türkiye. The residential building consists of five storeys with the total area of 2,120 m^2.

SolidWorks software was used to design the turbines, while ANSYS Fluent software was used to measure the turbine performance and the energy output of each turbine. Finally, DesignBuilder software was used to determine the energy reduction potential within the residential building for each type of wind turbine.

The three vertical axis wind turbine designs include the three-blade IceWind turbine and the three-blade helical turbine, using NACA 0021 airfoil. The final design is the combined turbine, with three helical blades centered on the three-blade IceWind.

Payback periods for each turbine type were calculated to provide a detailed overview of the economics and feasibility of each turbine for use in urban buildings.

5.2 Conclusion of the thesis

The following statements are drawn from the conclusion of the study:

1. The three-blade IceWind turbine type achieved 10.60 years payback period while contributing to a 22.93 % drop in energy demand.
2. The three-blade helical turbine achieved a payback period of 12.89 years while reducing energy consumption by 18.45 %.
3. The combined turbine produced the best performance with 10.49 years payback period and an energy saving of around 30.88 %.
4. Rated power output, maximum power coefficient, and tip speed ratio (TSR) for the VAWTs were found as follows:

- IceWind: 430 W and Cp = 0.17 at TSR 1.8.
- Helical: 350 W and Cp = 0.21 at TSR 2.
- Combined: 590 W and Cp = 0.31 at TSR 1.5.

5. All types of VAWTs are used in simulation under İzmir weather conditions with an average wind speed of around 7 m/s annually.

5.3 Suggestions for Future Work

The following suggestions are proposed for future work:

1. The use of different types of vertical turbines, such as the Savonius type, could be compared with the turbines used in this study, and it could verify whether the selected turbines would be the best solutions for this type of residential building in urban areas.
2. Simulate the vertical axis wind turbines and see how their efficiency affects other types of buildings such as hospitals, schools, offices, etc.
3. Simulating the turbines in other regions with different climates, such as North and Central Türkiye, and verifying the percentage of energy consumption reduction in those areas.
4. Using practical experiments and comparing them with the numerical verification to provide a comprehensive view of the relative differences between practical and numerical experiments.
5. Using other models in the numerical verification such as RNG k- ε turbulence model and comparing the results.

5.4 Published Papers from the Thesis

[a] C. Turhan and Y. A. S. Saleh, “A case study for small-scale vertical wind turbine integrated building energy saving potential”. *Journal of Building Design and Environment*, vol. 3, no. 1, pp. 28115, Mar. 2024.

[b] Y. A. S. Saleh, G. G. Akkurt, and C. Turhan, “Reconstructing energy-efficient buildings after a major earthquake in Hatay, Türkiye”. *Buildings,* vol. 14, pp. 2043, Jul. 2024.

[c] K. H. Suffer and Y. A. S. Saleh, “Numerical and experimental investigation of the aerodynamic for the IceWind blades VAWT”. *International Journal of*

Scientific Research in Science, Engineering and Technology, vol. 11, no. 4, pp. 139–146, Jul. 2024.

[d] Y. A. S. Saleh, M. C. Austin, C. Carpino, and C. Turhan, "Determining payback period and comparing two small-scale vertical axis wind turbines installed at the top of residential buildings". *International Journal of Architectural Engineering Technology,* vol. 11, pp. 1–16, Aug. 2024.

[e] Y. A. S. Saleh and C. Turhan, "Integration of a novel small-scale roof-mounted combined vertical axis wind turbine for energy-efficient buildings", presented at *15th Int. Exergy, Energy and Environment Symp. (IEEES-15),* Istanbul, Türkiye, Dec. 2024.

[f] Y. A. S. Saleh, M. Durak, and C. Turhan, "Enhancing urban sustainability with novel vertical-axis wind turbines: A study on residential buildings in Çeşme". *Sustainability,* vol. 17, pp. 3859, Apr. 2025.

REFERENCES

[1] İ. Bayram, F. Ümmetoğlu, O. C. Yılmaz, T. G. Özbalta, and Y. Yıldız, “The energy efficiency challenge for Turkish historical buildings”. *in Proc. 6th Int. Project and Construction Management Conf. (IPCMC2020),* 2020, pp. 1–10.

[2] C. Difiglio, B. Ş. Güray, and E. Merdan, *Turkey energy outlook 2020*. Sabancı University, Istanbul International Centre for Energy and Climate (IICEC), Istanbul, Turkey, 2020, pp. 327–377.

[3] M. Santamouris and K. Vasilakopoulou, “Present and future energy consumption of buildings: Challenges and opportunities towards decarbonisation”. e-*Prime - Advances in Electrical Engineering, Electronics and Energy,* vol. 1, pp. 1–32, 2021.

[4] S. S. Yildiz, “Determining wind energy potential using geographic information system functions: A case study in Balıkesir, Turkey”. *Applied Sciences,* vol. 13, pp. 9183, Aug. 2023.

[5] M. Casini, “Small vertical axis wind turbines for energy efficiency of buildings”. *Journal of Clean Energy Technologies,* vol. 4, no. 1, pp. 56–65, Jan. 2016.

[6] A. Akpınar, M. İ. Kömürcü, M. Kankal, İ. H. Özölçer, and K. Kaygusuz, “Energy situation and renewables in Turkey and environmental effects of energy use”. *Renewable and Sustainable Energy Reviews,* vol. 12, pp. 2013–2039, 2008.

[7] A. Gupta, U. Ali, H. A. Abderrahmane, and I. Janajreh, “Blade pitching in vertical axis wind turbines: A double multiple stream tube theoretical approach to performance enhancement”. *Heliyon,* vol. 11, pp. e42101, Jan. 2025.

[8] A. Hirschl and D. Österreicher, “Evaluation of the influences of different roof shapes on the flow properties and performance of small wind turbines”. *Journal of Mechanical Engineering – Problemy Mashynobuduvannia,* vol. 26, no. 2, pp. 24–33, 2023.

[9] K. Calautit and C. Johnstone, “State-of-the-art review of micro to small-scale wind energy harvesting technologies for building integration”. *Energy Conversion and Management: X,* vol. 20, pp. 100457, Sep. 2023.

[10] Z. Tasneem, A. A. Noman, S. K. Das, D. K. Saha, M. R. Islam, M. F. Ali, M. F. R. Badal, M. H. Ahamed, S. I. Moyeen, and F. Alam, “An analytical review on the evaluation of wind resource and wind turbine for urban application: Prospect and challenges”. *Developments in the Built Environment,* vol. 4, pp. 100033, Oct. 2020.

[11] A. R. Jha, *Wind turbine technology*. Boca Raton, FL: CRC Press, Taylor & Francis Group, 2011, pp. 31–78

[12] I. Gil-Ozoudeh, O. Iwuanyanwu, A. C. Okwandu, and C. S. Ike, “The role of passive design strategies in enhancing energy efficiency in green buildings”. *Engineering Science & Technology Journal,* vol. 3, no. 2, pp. 71–91, Dec. 2022.

[13] P. Sarir and M. Sharifzadeh, “Application of passive and active scenarios to a residential building in a dry and hot climate to achieve a positive energy building (PEB)”. *Heliyon,* vol. 10, pp. e30694, May 2024.

[14] L. K. Hendinata, N. A. Siddiq, A. I. R. Fikri, M. A. Suprapto, and R. Prilia, “Passive window energy performance in buildings: Modeling of apartment buildings in Indonesia”. *Journal of Artificial Intelligence in Architecture,* vol. 2, no. 2, pp. 1–12, Aug. 2023.

[15] M. Monis and A. Rastogi, “A review of passive design strategies for improving building energy performance”. *International Journal of Multidisciplinary Innovative Research,* vol. 2, no. 1, pp. 43–50, Jan. 2022.

[16] N. Al-Tamimi, “Passive design strategies for energy efficient buildings in the Arabian Desert”. *Frontiers in Built Environment,* vol. 7, pp. 1–11, Jan. 2022.

[17] A. Arsentev and A. Rymarov, “Using phase change materials (PCM) to reduce energy consumption in buildings”. *E3S Web of Conferences,* vol. 410, pp. 04005, 2023.

[18] M. Jaradat, H. Al Majali, C. Bendea, C. C. Bungau, and T. Bungau, “Enhancing energy efficiency in buildings through PCM integration: A study across different climatic regions”. *Buildings,* vol. 14, pp. 40, Dec. 2023.

[19] M. T. Bekele and C. Atakara, “Residential building energy conservation in Mediterranean climate zone by integrating passive solar and energy efficiency design strategies”. *Buildings,* vol. 13, pp. 1073, Apr. 2023.

[20] H. Huang, W. I. Binti Wan Mohd Nazib, Y. Yu, and Y. Wang, “Energy performance of a high-rise residential building retrofitted to passive building standard – A case study”. *Applied Thermal Engineering,* vol. 181, pp. 115902, Aug. 2020.

[21] K. Terashima, H. Sato, and T. Ikaga, “PV/T solar panel for supplying residential demands of heating/cooling and hot water with a lower environmental thermal load”. *Energy & Buildings,* vol. 297, pp. 113408, Jul. 2023.

[22] C. García-Gáfaro, C. Escudero-Revilla, I. Flores-Abascal, J. M. Hidalgo-Betanzos, and A. Erkoreka-González, “A photovoltaic forced ventilated façade (PV-FVF) as heat source for a heat pump: Assessing its energetical profit in nZEB buildings”. *Energy & Buildings,* vol. 261, pp. 111979, Feb. 2022.

[23] S. Aneli, R. Arena, G. M. Tina, and A. Gagliano, “Improvement of energy self-sufficiency in residential buildings by using solar-assisted heat pumps and thermal and

electrical storage”. *Sustainable Energy Technologies and Assessments,* vol. 60, pp. 103446, Sep. 2023.

[24] T. Alarmouty, Q. Jobran, and F. Sharaf, “The effective of geothermal energy in buildings: A case study in Madaba city in Jordan”. *International Journal of Engineering Research and Applications (IJERA),* vol. 10, no. 7 (Series-VII), pp. 28–35, Jul. 2020.

[25] X. Hu, Y. Xiang, H. Zhang, Q. Lin, W. Wang, and H. Wang, “Active–passive combined energy-efficient retrofit of rural residence with non-benchmarked construction: A case study in Shandong province, China”. *Energy Reports,* vol. 7, pp. 1360–1373, Mar. 2021.

[26] M. Ali, A. Gherissi, and Y. Altaharwah, “Experimental and simulation study on a rooftop vertical-axis wind turbine”. *Open Engineering,* vol. 13, pp. 1–9, 2023.

[27] K. Naik, A. Ianakiev, A. S. Galadanci, G. Cucca, Shubham, and M. Sun, “Evaluating the potential of wind and solar energy in achieving zero energy ratings in residential homes: A Nottingham case study”. *Smart Energy,* vol. 13, pp. 100129, Dec. 2023.

[28] A. Ibrahim, D. S. Dabai, M. M. Kwaifa, and G. D. Sani, “Performance investigation of building integrated hybrid vertical axis wind turbine for small scale power generation”. *International Journal of Scientific Development and Research (IJSDR),* vol. 7, no. 11, pp. 173–185, Nov. 2022.

[29] R. Afify, “Experimental studies of an IceWind turbine”. *International Journal of Applied Engineering Research,* vol. 14, no. 17, pp. 3633–3645, 2019.

[30] K. H. Suffer and Z. S. Jabar, “Numerical investigation of the aerodynamics performance of hybrid Icewind-Darrius turbine”. *International Journal of Engineering and Artificial Intelligence,* vol. 2, no. 3, pp. 9–15, Sep. 2021.

[31] H. Mansour and R. Afify, “Design and 3D CFD static performance study of a two-blade IceWind turbine”. *Energies,* vol. 13, pp. 5356, Oct. 2020.

[32] I. Al-Bahadly, “Building a wind turbine for rural home”. *Energy for Sustainable Development,* vol. 13, pp. 159–165, 2009.

[33] A. S. Bahaj, L. Myers, and P. A. B. James, “Urban energy generation: Influence of micro-wind turbine output on electricity consumption in buildings”. *Energy and Buildings,* vol. 39, pp. 154–165, 2007.

[34] C. Turhan and Y. A. S. Saleh, “A case study for small-scale vertical wind turbine integrated building energy saving potential”. *Journal of Building Design and Environment,* vol. 3, no. 1, pp. 28115, Mar. 2024.

[35] K. H. Suffer and Y. A. S. Saleh, “Numerical and experimental investigation of the aerodynamic for the IceWind blades VAWT”. *International Journal of Scientific Research in Science, Engineering and Technology,* vol. 11, no. 4, pp. 139–146, Jul. 2024.

[36] Y. A. S. Saleh, G. G. Akkurt, and C. Turhan, “Reconstructing energy-efficient buildings after a major earthquake in Hatay, Türkiye”. *Buildings,* vol. 14, pp. 2043, Jul. 2024.

[37] Y. A. S. Saleh, M. C. Austin, C. Carpino, and C. Turhan, “Determining payback period and comparing two small-scale vertical axis wind turbines installed at the top of residential buildings”. *International Journal of Architectural Engineering Technology,* vol. 11, pp. 1–16, Aug. 2024.

[38] W. T. Chong, M. Gwani, C. J. Tan, W. K. Muzammil, S. C. Poh, and K. H. Wong, “Design and testing of a novel building integrated cross axis wind turbine”. *Applied Sciences,* vol. 7, pp. 251, Mar. 2017.

[39] R. K. Kavade and P. M. Ghanegaonkar, “Performance analysis of small scale variable pitch vertical axis wind turbine”. *FME Transactions,* vol. 50, no. 2, pp. 322–330, 2022.

[40] N. M. Ali, S. Aljabair, and A. H. A. Kareem, “An experimental and numerical investigation on Darrieus vertical axis wind turbine types at low wind speed”. *International Journal of Mechanical & Mechatronics Engineering (IJMME-IJENS),* vol. 19, no. 6, pp. 97–110, Dec. 2019.

[41] D. Redchyts, K. Portal-Porras, S. Tarasov, S. Moiseienko, U. Tuchyna, N. Starun, and U. Fernandez-Gamiz, “Aerodynamic performance of vertical-axis wind turbines”. *Journal of Marine Science and Engineering,* vol. 11, pp. 1367, Jul. 2023.

[42] U. Divakaran, A. Ramesh, A. Mohammad, and R. K. Velamati, “Effect of helix angle on the performance of helical vertical axis wind turbine”. *Energies,* vol. 14, pp. 393, Jan. 2021.

[43] L. P. Issac, S. Shivakumar, V. Umesh, S. Jangam, N. Santhosh, G. Shankar, and B. A. Praveen, “The design and analysis of helical cross-axis wind turbine”. *AIP Conference Proceedings,* vol. 2421, pp. 020004, Jan. 2022.

[44] A. B. Suresh, C. P. Selvan, N. Vinayaka, M. P. G. Chandrashekarappa, A. Lakshmikanthan, R. Rangappa, S. Shinde, and V. R. Malik, “Computational investigations of aluminum based airfoil profiles of helical shaped vertical axis wind turbines suitable for friction stir joining and processing”. *International Journal on Interactive Design and Manufacturing (IJIDeM),* vol. 17, pp. 1091–1111, 2023.

[45] D. Han, Y. G. Heo, N. J. Choi, S. H. Nam, K. H. Choi, and K. C. Kim, “Design, fabrication, and performance test of a 100-W helical-blade vertical-axis wind turbine at low tip-speed ratio”. *Energies,* vol. 11, pp. 1517, Jun. 2018.

[46] G. Mohammed, A. Ibrahim, U. M. Kangiwa, and B. W. Joshua, "Design and testing of building integrated hybrid vertical axis wind turbine". *Journal of Electrical and Electronic Engineering,* vol. 9, no. 3, pp. 69–77, Jun. 2021.

[47] T. Gad, A. Shokry, R. Afify, E. Saber, and M. Hassan, "Experimental study of two, two-reversed, three and four blade IceWind turbine". *International Journal of Applied Engineering Research*, vol. 15, no. 12, pp. 1122–1134, Dec. 2020.

[48] Z. Lillahulhaq, A. Muchyiddin, R. W. Suhadak, I. Amirullah, F. D. Sandy, and A. C. Embot, "Experimental study wind turbine performance of Straight-Savonius and Ice-Wind type on the similar proportion aspect ratio". *Journal of Physics: Conference Series*, vol. 2117, pp. 012008, 2021.

[49] M. Zheng, Y. Li, H. Teng, J. Hu, Z. Tian, and Y. Zhao, "Effect of blade number on performance of drag type vertical axis wind turbine". *Applied Solar Energy,* vol. 52, no. 4, pp. 315–320, 2016.

[50] I. Karadag and I. Yuksek, "Wind turbine integration to tall buildings" *in Renewable Energy - Resources, Challenges and Applications,* 1st ed. London, UK: IntechOpen, Sep. 2020, pp. 1–15.

[51] M. Kottek, J. Grieser, C. Beck, B. Rudolf, and F. Rubel, "World map of the Köppen-Geiger climate classification updated". *Meteorologische Zeitschrift,* vol. 15, no. 3, pp. 259–263, Jun. 2006.

[52] F. Ayhan and H. Yazıcı, "İzmir ili nüfusunun gelişimi ve değişimine dair demografik analiz çalışması". *USOBED Uluslararası Batı Karadeniz Sosyal ve Beşerî Bilimler Dergisi,* vol. 7, no. 2, pp. 273–290, Dec. 2023.

[53] İzmir Development Agency, "Wind energy sector in İzmir". Internet: https://www.investinizmir.com, 2023 [Nov. 2024].

[54] Global Wind Atlas. Internet: https://globalwindatlas.info/ar [Nov. 2024].

[55] Türk Standardları Enstitüsü (TSE), "TS 825 - Binalarda ısı yalıtım kuralları [Thermal insulation requirements for buildings]". Internet: https://www.tse.org.tr, May 2008 [Nov. 2024].

[56] Ankara Büyükşehir Belediyesi, "Ankara Büyükşehir Belediyesi İmar Yönetmeliği [Ankara Metropolitan Municipality Zoning Regulation]". Internet: https://www.ankara.bel.tr, 2023 [Nov. 2024].

[57] DesignBuilder, DesignBuilder Software, version 7.0.2.006. Internet: http://www.designbuilder.co.uk/ [Sep. 2, 2024].

[58] SolidWorks, SolidWorks 2018. Internet: https://www.solidworks.com/ [May 10, 2024].

[59] International Electrotechnical Commission (IEC), *IEC 61400-2: Wind turbines – Part 2: Design requirements for small wind turbines*, 2nd ed. Geneva, Switzerland: IEC, Mar. 2006.

[60] ANSYS, ANSYS Fluent, 2020. Internet: https://www.ansys.com/ [May 10, 2024].

[61] N. Durrani, N. Qin, H. Hameed, and S. Khushnood, "2-D numerical analysis of a VAWT wind farm for different configurations," *in Proc. of the 49th AIAA Aerospace Sciences Meeting including the New Horizons Forum and Aerospace Exposition*, Orlando, FL, USA, Jan. 2011, pp. 1–10.

[62] E. Singh, S. Roy, K. S. Yam, and M. C. Law, "Numerical analysis of H-Darrieus vertical axis wind turbines with varying aspect ratios for exhaust energy extractions". *Energy*, vol. 277, pp. 127739, May 2023.

[63] A. Eltayesh, F. Castellani, F. Natili, M. Burlando, and A. Khedr, "Aerodynamic upgrades of a Darrieus vertical axis small wind turbine". *Energy for Sustainable Development*, vol. 73, pp. 126–143, Feb. 2023.

[64] I. F. Zidane, H. M. Ali, G. Swadener, Y. A. Eldrainy, and A. I. Shehata, "Effect of upstream deflector utilization on H-Darrieus wind turbine performance: An optimization study". *Alexandria Engineering Journal*, vol. 63, pp. 175–189, 2023.

[65] R. Ansaf, H. S. Abdelhameed, I. Hashem, and Z. Harun, "Efficiency-based design optimization of the H-type Darrieus wind turbine with fixed guiding-walls". *Energy Reports*, vol. 9, pp. 3576–3592, Feb. 2023.

[66] S. ed-Dîn Fertahi, A. Samaouali, and I. Kadiri, "CFD comparison of 2D and 3D aerodynamics in H-Darrieus prototype wake". *e-Prime – Advances in Electrical Engineering, Electronics and Energy*, vol. 4, pp. 100178, May 2023.

[67] A. Azmi, A. H. Sebayang, and A. Harjon, "Life cycle cost analysis and payback period of 12-kW wind turbine for a remote telecommunications base station in Malaysia". *Aceh International Journal of Science and Technology*, vol. 12, no. 2, pp. 304–316, Aug. 2023.

[68] L. F. S. Fonseca and M. Carvalho, "Greenhouse gas and energy payback times for a wind turbine installed in the Brazilian Northeast". *Frontiers in Sustainability*, vol. 3, pp. 1060130, Dec. 2022.

[69] ANSYS, Inc., *Ansys Fluent Theory Guide*, Release 2021 R2. Canonsburg, PA, USA: ANSYS, Inc., Jul. 2021.

[70] C. Turhan and G. G. Akkurt, "Assessment of thermal comfort preferences in Mediterranean climate: A university office building case". *Thermal Science*, vol. 22, no. 5, pp. 2177–2187, 2018.